Title: E3 ubiquitin ligase Listerin regulates macrophage cholesterol efflux and atherosclerosis by targeting ABCA1

Authors: Lei Cao[1#], Jie Zhang[1#], Liwen Yu[1#], Wei Yang[1], Wenqian Qi[1], Ruiqing Ren[1], Yapeng Liu[1], Yonghao Hou[1], Yu Cao[1], Qian Li[1], Xiaohong Wang[1], Zhengguo Zhang[2], Bo Li[3], Wenhai Sui[1,4], Yun Zhang[1,4], Chengjiang Gao[5]*, Cheng Zhang[1,4]*, Meng Zhang[1,4]*

Affiliations:

[1] State Key Laboratory for Innovation and Transformation of Luobing Theory; Key Laboratory of Cardiovascular Remodeling and Function Research, Chinese Ministry of Education, Chinese National Health Commission and Chinese Academy of Medical Sciences; Department of Cardiology, Qilu Hospital of Shandong University, Jinan, China

[2] Organ Procurement Organizations, Qilu Hospital of Shandong University, Jinan, Shandong, China

[3] Department of Cardiology, Zibo Central Hospital, Zibo, Shandong, China

[4] Cardiovascular Disease Research Center, Jinan Central Hospital, Shandong First Medical University, Jinan, Shandong, China

[5] Key Laboratory of Infection and Immunity of Shandong Province, Department of Immunology, Cheeloo College of Medicine, Shandong University, Jinan, China

Address correspondence to: Meng Zhang, Department of Cardiology, Qilu Hospital of Shandong University, No. 107, Wenhua West Road, Jinan 250012, Shandong, China. Phone: 86.531.8216.9263; Email: zhangmeng@sdu.edu.cn. Cheng Zhang, Department of Cardiology, Qilu Hospital of Shandong University, No. 107, Wenhua West Road, Jinan 250012, Shandong,

China. Phone:86.531.8216.9411; Email: zhangc@sdu.edu.cn. Chengjiang Gao, Department of Immunology, Cheeloo College of Medicine, Shandong University, No. 44, Wenhua West Road, Jinan 250012, Shandong, China. Phone:86.531.8838.2292; Email:cgao@sdu.edu.cn.

Conflict-of-interest statement：The authors have declared that no conflict of interest exists

Abstract: Atherosclerosis arises from disrupted cholesterol metabolism, notably impaired macrophage cholesterol efflux leading to foam cell formation. Through single-cell and bulk RNA sequencing, we identified Listerin as a regulator of macrophage cholesterol metabolism. Listerin expression increased during atherosclerosis progression in humans and rodents. Its deficiency suppressed cholesterol efflux, promoted foam cell formation, and exacerbated plaque features (macrophage infiltration, lipid deposition, necrotic cores) in macrophage-specific knockout mice. Conversely, Listerin overexpression attenuated these atherosclerotic manifestations. Mechanistically, Listerin stabilizes ABCA1, a key cholesterol efflux mediator, by catalyzing K63-linked polyubiquitination at residues K1884/K1957, countering ESCRT-mediated lysosomal degradation of ABCA1 induced by oxLDL. ABCA1 agonist Erythrodiol restored cholesterol efflux in Listerin-deficient macrophages, while ABCA1 knockout abolished Listerin's effects in THP-1 cells. This study establishes Listerin as a protective factor in atherosclerosis via post-translational stabilization of ABCA1, offering a potential therapeutic strategy targeting ABCA1 ubiquitination to enhance cholesterol efflux.

Graphical abstract

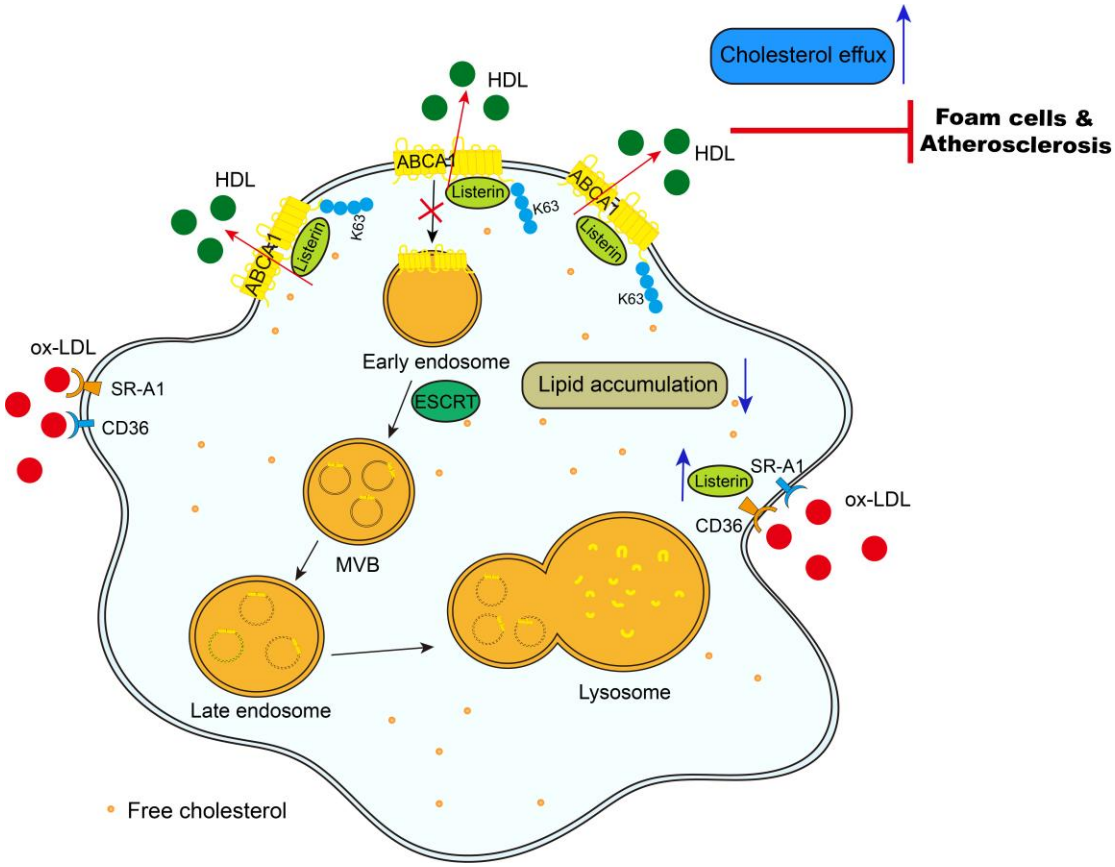

Main Text:

INTRODUCTION

Atherosclerotic cardiovascular disease (ASCVD) is the leading cause of morbidity and mortality worldwide (1-4). Atherosclerosis is characterized by excessive lipid deposition in the intima of the arterial wall, and macrophages play key roles in this process (2, 5-7). Monocytes in the blood enter the subintima to differentiate into macrophages and phagocytose-modified lipoproteins (8-11). In persistent hyperlipidemia, macrophages become foam cells and constitute the core of the atherosclerotic plaque (4, 9, 12). Unstable plaques progress to plaque rupture and thrombosis, leading to acute myocardial ischemia and myocardial infarction (10). Although macrophage foam cell formation plays an indispensable role in atherosclerosis, the underlying molecular mechanisms have not been fully elucidated.

ATP-binding cassette transporter A1 (ABCA1) is an integral membrane protein with a molecular weight of 254 kDa and is expressed on the plasma and endosomal membranes of many tissues (13-17). ABCA1 promotes the efflux of plasma membrane free cholesterol and phospholipids to apolipoprotein A-1 (ApoA1) and forms nascent high-density lipoprotein (HDL) (18, 19). Numerous studies have shown that ABCA1 plays an essential role in reverse cholesterol transport (RCT) in macrophages by stimulating the efflux of cholesterol, thereby reducing foam cell formation and the progression of atherosclerosis (20, 21). As a membrane protein, ABCA1 was also reported to be degraded through the endosomal sorting complex required for the transport (ESCRT)-lysosome pathway (22). Ubiquitination is an important post-translational modification of proteins and is widely involved in protein degradation, stability, translocation, and signaling pathway activation (23). However, the regulatory

mechanisms underlying ABCA1 translocation and protein stability, especially associated with ubiquitination, has not yet been fully revealed.

Listerin is an important member of the E3 ubiquitin ligase family with a typical RING domain, and it's homologue LTN1 in yeast was reported to play an important role in regulating aberrant nascent polypeptides for proteasomal degradation. However, the role of Listerin in mammals and disease progression deserves further study. Macrophages internalize oxLDL through scavenger receptors (e.g., CD36, SRA1). When their lipoprotein engulfing capacity surpasses cholesterol efflux mechanisms—a hallmark of disrupted cholesterol homeostasis—these macrophages undergo phenotypic transition to foam cells, which subsequently drive the formation of the lipid-rich necrotic core characteristic of advanced atherosclerotic plaques. To investigate potential molecular regulators of this pathogenic cascade, we conducted transcriptomic profiling and identified *Listerin* as a significantly up-regulated E3 ligase in cholesterol ester stimulated macrophages. Furthering examined the role of Listerin in atherosclerosis, we conducted a series of molecular biology experiments we found that Listerin can bind to ABCA1 to catalyze its K63-linked ubiquitination at Lys1884 and Lys1957, which inhibits lysosomal degradation via the ESCRT-lysosome pathway. Our study identified the E3 ubiquitin ligase Listerin as a regulator of ABCA1 translocation from the cytomembrane and protein stability. We also found that this modification plays an important role in reducing lipid deposition in macrophages and the progression of atherosclerosis.

RESULTS

Listerin expression increases in human and mouse atherosclerotic plaque tissues

Macrophage transition into foam cells under cholesterol ester accumulation drives atherosclerotic pathogenesis(24-26). To identify ubiquitination-related regulators of this process, we first performed RNA sequencing on oxLDL-treated THP-1-derived macrophages alongside reanalysis of peripheral blood mononuclear cells (PBMC) transcriptomes from carotid atherosclerosis patients (GSE23746). Both datasets revealed *Listerin* upregulation in foam cells and patient monocytes (Figure S1, A and B). To further explore the role of macrophage Listerin in atherosclerosis, we analyzed the time-series scRNA-seq data (GSE155513) and revealed cellular heterogeneity during the development of atherosclerotic plaque. There were four time points of plaque progression (Figure S1C) including 0 weeks group (0W), 8 weeks group (8W), 16 weeks group (16W), and 26 weeks group (26W). Unbiased clustering of 28687 cells from all samples revealed 18 clusters (Figure S1C). Based on established lineage-specific marker genes (Figure S1D), these clusters were assigned to seven cell lineages, including ECs (*Pecam1, Cdh5*), VSMCs (*Tagln, Acta2*), fibroblasts (*Serpinf1, Pdgfra*), and Macrophage (*C1qa, Cd68*), among others (Figure 1A). The proportions of different cell types showed significant variations with the progression of atherosclerotic plaque (Figure S1E). This includes transformations of smooth muscle cells and increased neutrophil infiltration, among other changes (Figure S1F). Notably, the macrophage (Mφ) obviously increased with further aggravation of atherosclerotic plaques, whether in quantity or proportion (Figure 1B, Figure S1F). Intriguingly, *Listerin* expression within macrophages demonstrated progressive elevation across plaque development (Figure 1, B and C), a pattern

concordant with upregulated levels observed in human atherosclerotic plaques (GSE57691) and patient-derived PBMC (GSE23746) (Figure 1, D and E). Therefore, above results indicated that macrophage Listerin may be related to atherosclerosis progression.

To further investigate the association between macrophage Listerin and atherosclerosis, we measured the expression of Listerin in coronary atherosclerotic plaque and found a strong positive correlation between macrophage Listerin and plaque progression (i.e., pathological intimal thickening [PIT], fibroatheroma) (Figure 1F, Figure S1G). Suggesting that Listerin play an important role in the development of atherosclerosis. Parallel investigations in atherosclerotic mouse models (fed a WD for different durations) recapitulated this trend, with aortic Listerin expression significantly elevated in late-stage lesions characterized by dense macrophage infiltration (Figure 1G). This observation was further corroborated by immunoblotting analysis of whole aortic lysates, which confirmed the upregulation of Listerin protein levels (Figure 1H). To further investigate the regulatory effect of oxLDL stimulation (a risk factor for atherosclerosis) on Listerin expression in macrophages, we isolated primary peritoneal macrophages (PMs). Following oxLDL stimulation, immunofluorescence assays demonstrated a time-dependent upregulation of Listerin expression in PMs (Figure S1H). Subsequent immunoblotting (Figure 1I) and quantitative RT-PCR analyses (Figure 1J) demonstrated significant increases in both protein and transcript levels of Listerin in oxLDL-treated PMs. Importantly, these findings were recapitulated in RAW264.7 macrophage cell lines, with parallel experiments showing consistent elevation of Listerin protein (Figure S1I) and mRNA expression (Figure S1J) under identical stimulation conditions. Taken together,

these data suggest that Listerin is involved in the development of atherosclerosis and plays a potential role in this disease.

Macrophage Listerin deficiency inhibits cholesterol efflux and aggravates foam cell formation

Macrophages exhibit functional plasticity during atherogenesis, dynamically engaging in lipid handling and inflammatory responses. To delineate Listerin's spatial regulation, we performed a more detailed subtyping of macrophages (Figure 2A) and found that Listerin-positive macrophages were primarily concentrated in the TREM2hi macrophage subtype, and their proportion significantly increased with disease progression (Figure 2B). Gene ontology analysis further associated Listerin-expressing macrophages with lipid transport and cholesterol efflux signatures (Figure 2C), suggesting a potential role in cholesterol homeostasis. To functionally validate these observations, we generated macrophage-specific Listerin knockout mice (Listerin$^{fl/fl}$Lyz2^{cre}) via Cre-lox recombination to conditionally knock out–exons 3-5 of the Listerin gene (Figure S2A). Effective knockout was confirmed by extracting PMs from Listerin$^{fl/fl}$ and Listerin$^{fl/fl}$Lyz2^{cre} mice (Figure S2B).

Based on the aforementioned single-cell sequencing data, we next investigated the effects of Listerin on cholesterol metabolism and foam cell formation in detail. Oil Red O staining revealed exacerbated lipid accumulation in Listerin-deficient PMs under oxLDL stimulation (Figure 2D). Conversely, adenoviral overexpression of wild-type Listerin – but not its E3 ligase-deficient mutant (ΔRING) – attenuated foam cell formation in PMs (Figure 2, E and F, Figure S2C). Furthermore, we restored Listerin protein expression in Listerin-deficient PMs through adenovirus infection. Reconstitution of Listerin restored lipid deposition upon

stimulation with oxLDL, whereas the truncated mutant Listerin-ΔRing did not (Figure S2D). These findings position Listerin as a ubiquitination-dependent regulator of macrophage lipid metabolism.

Given the established paradigm that foam cell formation stems from disrupted cholesterol efflux-lipoprotein uptake equilibrium(27-29). To systematically dissect Listerin's mechanistic contribution, we stimulated PMs with fluorescently labeled oxidized low-density lipoprotein (Dil-oxLDL). While Listerin deficiency did not impair modified lipoprotein uptake capacity in PMs (Figure 2G). Concurrently, de novo lipogenesis assays revealed no significant alteration in lipid synthesis pathways in Listerin-deficient macrophages (Figure S2E). These combined observations prompted us to hypothesize that Listerin might regulate cholesterol efflux mechanisms rather than influencing lipoprotein uptake or lipid biosynthesis processes. Cholesterol efflux from plaque macrophages is also known as RCT, which plays a key role in foam cell formation (12, 30-33) by reducing lipid deposition of macrophages in atherosclerotic lesions. Thus, we first investigated the effects of Listerin on cholesterol efflux in vitro. The result showed that Listerin deficiency resulted in the accumulated NBD-cholesterol in the PMs was significantly increased (Figure 2H), and a time-dependent reduction of cholesterol efflux to apolipoprotein-A1 (ApoA1) (Figure S2F, Figure 2I). Accordingly, cholesterol efflux was detected in Listerin-overexpressing PMs. Listerin overexpression promoted cholesterol efflux to ApoA1, but not its E3 ligase-deficient mutant (ΔRING) (Figure 2J). Furthermore, we found that reconstitution of Listerin in Listerin-deficient PMs restored cholesterol efflux in a RING domain-dependent manner (Figure S2G), mirroring the foam cell formation phenotypes. Next, we investigated the effect of Listerin deficiency on RCT *in vivo*. RAW 264.7 macrophages

transfected with control or Listerin siRNA were loaded with oxLDL and transplanted into the peritoneal cavity of mice. The amount of labeled cholesterol exported from macrophages with Listerin knockdown to plasma, liver, and feces was reduced compared to that of control macrophages (Figure 2K). Altogether, these findings suggest that Listerin can reduce the lipid accumulation by promoting cholesterol efflux, thereby ameliorating macrophage-derived foam cell formation.

Macrophage Listerin deficiency promotes lipid accumulation and foam cell formation through downregulating ABCA1 expression

To delineate the molecular mechanism underlying Listerin-mediated cholesterol efflux, we performed quantitative proteomics in macrophages isolated from Listerin-deficient mice and control mice (Figure 3A). This analysis identified ABCA1–a master regulator of cholesterol transport–was significantly downregulated upon Listerin ablation (Figure 3B). To verify the proteomics results, we examined some lipid endocytosis-associated receptors such as the class A1 scavenger receptor (SRA1), CD36, and CD68 (34). Cholesterol efflux receptors, ABCA1, ATP-binding cassette transporter G1 (ABCG1), and scavenger receptor type B class I (SRB1) were also analyzed (30). Interestingly, following oxLDL stimulation, Listerin deficiency significantly reduced ABCA1 protein expression in PMs, while other receptors remained unaffected (Figure 3C). Notably, *ABCA1* mRNA levels showed no alterations (Figure S3A), suggesting that Listerin regulates ABCA1 at the post-transcriptional level. Additionally, Cycloheximide chase assays demonstrated accelerated ABCA1 degradation in knockout macrophages, establishing Listerin's role in post-translational stabilization (Figure 3D). Consistently, we next isolated PBMC from both control subjects and ASCVD patients, and

differentiated them into peripheral blood monocyte-derived macrophages (MDMs) using macrophage colony-stimulating factor (M-CSF). RNA interference-mediated knockdown of Listerin in these cells demonstrated significant downregulation of ABCA1 expression (Figure 3E). This finding was recapitulated in bone marrow-derived macrophages (BMDM) from Listerin-knockout mice, which showed concordant reduction in ABCA1 protein levels (Figure S3B). On the contrary, adenovirus-mediated overexpression of Listerin, but not of Listerin-ΔRing, increased ABCA1 protein expression in PMs (Figure 3F). Furthermore, reconstitution of Listerin in knockout PMs restored oxLDL-induced ABCA1 expression, whereas the catalytically inactive Listerin-ΔRing mutant failed to rescue this phenotype (Figure S3C), establishing a strict structure-function relationship between Listerin's E3 ligase activity and ABCA1 stabilization.

To establish causality between Listerin-ABCA1 axis dysfunction and foam cell formation, we employed pharmacological and genetic approaches. Erythrodiol is a selective inhibitor for ABCA1 protein degradation, and our results confirmed that Erythrodiol could up-regulate the expression of ABCA1 protein without affecting the expression of ABCG1 and SRB1 (Figure S3D). Then, cholesterol efflux and foam cell formation were investigated in PMs isolated from Listerin$^{fl/fl}$ and Listerin$^{fl/fl}$Lyz2^{cre} mice and the results indicated that Listerin deficient PMs had significantly increased foam cell formation and inhibited cholesterol efflux, which was abrogated specifically by pre-treatment using ABCA1 agonist Erythrodiol (Figure 3G, Figure S3, E and F). Crucially, we constructed an ABCA1 knockout THP-1 cell using the CRISPR/Cas9 system and found that Listerin deficiency did not further increase lipid deposition in ABCA1-KO cells (Figure 3H). These findings collectively position Listerin as a

ubiquitin-dependent stabilizer of ABCA1, orchestrating macrophage cholesterol efflux to mitigate foam cell pathogenesis.

Listerin inhibits the degradation of ABCA1 through the ESCRT-lysosomal pathway

ABCA1 protein degradation has a precise regulatory mechanism, and excessive or misfolded ABCA1 may be degraded. Notably, ABCA1 protein degradation includes two important pathways: the calpain-mediated degradation pathway (35, 36) and the ubiquitin-mediated degradation pathway (22). Ubiquitin-mediated degradation of ABCA1 can be divided into lysosomal and non-lysosomal pathways (37). Ubiquitin is mostly considered as a sorting protein for proteasome degradation. A growing body of evidence shows that this molecule also labels membrane proteins for lysosomal degradation, in which the ESCRT pathway serves as a dominant mechanism (22, 38, 39). Disruption of ESCRT significantly delays the degradation of cell surface-resident ABCA1 (22).

To define Listerin's role in ABCA1 regulation, we carried out a series of experiments, and the results showed that the protein degradation of ABCA1 in Listerin-deficient PMs was restored by the lysosomal inhibitors chloroquine, NH_4Cl and bafilomycin A1 (BafA1), but not by the proteasome inhibitor MG132 or calpain inhibitor calpeptin (Figure 4, A and B). In conclusion, the loss of Listerin in macrophages mediated ABCA1 degradation through lysosomes. Next, we treated Listerin-deficient PMs with the autophagy inhibitor 3-MA and wortmannin, or the ESCRT inhibitor DBeQ which blocking Multivesicular Bodies (MVBs) formation to investigate lysosomal sorting mechanisms. Unexpectedly, the degraded ABCA1 was restored by DBeQ (Figure 4B). We also designed a specific siRNA for hepatocyte growth factor-regulated tyrosine kinase substrate (HRS), which is a subunit of ESCRT-0 that plays an

important role in the ESCRT system (38, 40), and the expression of endogenous HRS was significantly lower (Fig. S4A). The results showed that the degradation of ABCA1 protein by Listerin-deficient in PMs was restored after HRS-specific siRNA application (Figure S4B). Collectively, these findings provide initial evidence that Listerin deficiency accelerates ABCA1 degradation via the ESCRT-dependent lysosomal sorting machinery.

To further verify the correlation between ESCRT system and ABCA1 degradation, we used the CRISPR/Cas9 system to knock out HRS in THP-1 cells. Consistently, the decrease in ABCA1 protein expression and cholesterol efflux resulting from Listerin deficiency were restored after HRS deletion (Figure 4, C and D). In contrast, ATG5 [an essential autophagy-related protein, which regulates autophagy formation (41)] KO THP-1 cells still showed decrease ABCA1 expression and cholesterol efflux after Listerin deficiency (Figure 4, E and F). Similar results were observed in HRS-KO or ATG5-KO HEK293T cells (Figure S4, C and D). Mechanistic interrogation revealed that Listerin deficiency increased ABCA1-HRS binding despite reducing total ABCA1 levels (Figure 4G), whereas Listerin overexpression diminished this interaction in both co-immunoprecipitation (Figure S4E) and immunofluorescence assays (Figure 4H). Parallel lysosomal tracking demonstrated enhanced ABCA1 accumulation in lysosomes upon Listerin knockout (Figure S4F). These complementary approaches demonstrate that Listerin stabilizes ABCA1 by blocking its recognition by the ESCRT complex, thereby preventing lysosome-mediated degradation.

Beyond stabilizing ABCA1 protein levels, Listerin was found to regulate ABCA1 membrane dynamics, and thus cell surface-resident ABCA1 was investigated. We used flow cytometry to examine the changes in ABCA1 expression on the cell membrane after Listerin

knockout. The results showed that the fluorescence intensity of membrane ABCA1 was significantly reduced in Listerin-deficient macrophages (Figure 4I), whereas overexpression of Listerin significantly enhanced the fluorescence intensity of membrane ABCA1 (Figure S4, G and H). Complementally, we extracted cell surface-resident proteins from PMs of Listerin$^{fl/fl}$ and Listerin$^{fl/fl}$Lyz2^{cre} mice. Western blotting (Figure 4J) and immunofluorescence (Figure 4K) analyses demonstrated preferential degradation of membrane-resident ABCA1 over total cellular pools in knockout cells. Notably, HRS knockdown reversed this surface depletion, as evidenced by restored membrane ABCA1 in both immunofluorescence (Figure 4K) and immunoblot analyses (Figure S4I). These findings collectively demonstrate Listerin's role in preserving ABCA1 membrane residency by blocking ESCRT-mediated lysosomal sorting.

Although yeast LTN1 (Listerin homolog) participates in ribosome-associated quality control (RQC) through proteasomal targeting of aberrant polypeptides (42-44), genetic disruption of RQC via NEMF knockdown -the central player of RQC system (44, 45) - failed to rescue ABCA1 degradation in Listerin-deficient macrophages (Figure S4, J and K). CRISPR-engineered NEMF knockout THP-1 cells similarly maintained ABCA1 loss and cholesterol efflux defects upon Listerin deletion (Figure S4, L and M), confirming mechanistic independence from RQC pathways. This multi-tiered analysis establishes Listerin as a specialized regulator of ABCA1 trafficking, operating through ESCRT-lysosomal inhibition rather than canonical quality control mechanisms.

Listerin targets ABCA1

To elucidate the structural basis of Listerin-ABCA1 interaction, we performed systematic domain mapping experiments. Time-gradient co-immunoprecipitation (Co-IP) assays in

oxLDL-stimulated PMs revealed progressive enhancement of endogenous Listerin-ABCA1 binding (Figure 5A), consistent with prior observations of cholesterol-dependent transporter regulation. Specificity analysis in HEK293T cells demonstrated Listerin exclusively co-precipitated with ABCA1, but not with ABCG1 or SRB1 (Figure 5B, Figure S5A), while confocal microscopy confirmed their membrane colocalization under atherogenic conditions (Figure 5C). To further validate the clinical association between Listerin and ABCA1 in human macrophage. We performed flow cytometric analysis of PBMC isolated from control subjects and ASCVD patients and revealed a marked upregulation of both Listerin and ABCA1 expression in CD11b+ monocyte subsets (Figure 5, D and E). This expression profile was further validated in PBMC of control subjects and ASCVD patients, where ASCVD-derived PBMC exhibited higher Listerin and ABCA1 protein levels compared to controls (Figure S5B). Complementing these cellular findings, multiparametric immunofluorescence analysis of human coronary artery plaques demonstrated coordinated upregulation of both Listerin and ABCA1 proteins in plaque-associated macrophages during atherosclerotic progression (Figure 5, F and G). These findings suggest a robust correlation between Listerin and ABCA1 in macrophages, indicating that Listerin likely modulates foam cell formation through its regulatory effects on ABCA1. Then, Dose-dependent overexpression in HEK293T cells confirmed Listerin-mediated ABCA1 stabilization (Figure S5C), abrogated by catalytic mutants -Listerin-ΔRing and Listerin-C/A (Figure S5D), implicating ubiquitination-dependent regulation.

To explore the binding domains of ABCA1 that are necessary for its interaction with Listerin, several GFP-ABCA1 truncated mutants were constructed, including the deletion

mutants GFP-ABCA1-ΔN1R1 (in which the NBD1, RD1 domains were deleted), GFP-ABCA1-ΔN2R2 (in which the NBD2 and RD2 domains were deleted), and GFP-ABCA1-ΔNRNR (in which the full NBD/RD domains were deleted) (Figure 5H), and some other truncated plasmids, such as GFP-ABCA1-RD1, RD2, NBD1, and NBD2 (Figure 5J). Co-IP and immunofluorescence experiments show that the binding of ΔN1R1 and ΔN2R2 mutants to Listerin were significantly reduced, while the ΔNRNR mutant almost completely loses Listerin interaction (Figure 5I, Figure S5E). Importantly, both GFP-ABCA1-RD2 (containing only the RD2 domain) and GFP-ABCA1-NBD1 (containing only the NBD1 domain) maintained effective co-precipitation with Flag-Listerin (Figure 5K). Based on these results, we conclude that Listerin interacts with RD2 and NBD1 domains of ABCA1, modulating its stability through spatially defined ubiquitination to regulate cholesterol efflux.

Listerin catalyzes K63-linked polyubiquitination of ABCA1 at the residues Lys1884 and Lys1957 to inhibit foam cell formation

Ubiquitination is a crucial post-translational modification of proteins that are involved in protein degradation, stability, translocation, and signaling pathway activation (23). ABCA1 can be ubiquitinated, followed by proteasomal and lysosomal degradation (37). Building on the established interaction between Listerin and ABCA1, we investigated its enzymatic role in ABCA1 ubiquitination. Co-expression of Listerin with ABCA1 and ubiquitin variants in HEK293T cells revealed preferential induction of K63-linked (vs. K48-linked) polyubiquitination, dependent on intact E3 ligase activity (Figure 6, A and B). This pattern was recapitulated endogenously, with Listerin knockout macrophages showing reduced ABCA1 K63-ubiquitination without affecting K48-linked modifications (Figure 6C). Furthermore, we

performed tandem ubiquitin-binding entities (TUBEs) pull-down assays to purify the ubiquitinated substrates. Western blotting analyses showed that the polyubiquitination of ABCA1 was reduced in Listerin-deficient macrophages (Figure 6D).

To determine the lysine residues of ABCA1 responsible for Listerin-mediated polyubiquitination, we performed liquid chromatography-mass spectrometry (LC-MS) analysis with HEK293T cells, in which GFP-ABCA1 was co-transfected with Flag-Listerin and HA-ubiquitin, or GFP-ABCA1 only with HA-ubiquitin. Comparative analysis revealed two intracellular lysine residues (K1884 and K1957) demonstrating high-confidence scores and changed significantly after overexpression of Listerin compared to basal conditions (Figure 6E). Following, we performed precise structural localization of these ubiquitination sites by integrating ABCA1 cryo-EM structure (PDB:7TBY) with AlphaFold2 predictions (Figure S5F). Based on these results, we constructed the ABCA1 mutants K1884R and K1957R, in which the lysine residues were replaced with arginine. At the same time, we also constructed the ABCA1 mutants K1314R, K1189R, and K2023R according to the LC-MS analysis to verify whether other lysine sites participated in Listerin mediated ABCA1 ubiquitination. Subsequently, the mutants were transfected into HEK293T cells and analysis revealed that Listerin-mediated K63-linked polyubiquitination of ABCA1 increased significantly in cells containing the K1314R, K1189R, and K2023R mutants (Figure S5G). However, in the K1884R and K1957R mutants, Listerin-mediated polyubiquitination of K63-linked ABCA1 increased slightly. Notably, mutations at both loci (K1884R and K1957R) restored K63-linked ubiquitination of ABCA1 mediated by Listerin (Figure 6F). Functional studies in RAW264.7 macrophages demonstrated loss of Listerin's lipid-reducing effects when expressing these

ABCA1 mutants, evidenced by unabated Oil Red O staining (Figure 6, G and H), unchanged ABCA1 protein levels (Figure 6I), and impaired cholesterol efflux rescue (Figure 6J). Correspondingly, in the in vivo RCT experiments, due to the K1884 and K1957 mutations in ABCA1, Listerin was unable to continue promoting the ubiquitination and stabilization of ABCA1. As a result, the cholesterol efflux capacity of ABCA1-K1884/K1957 was weakened compared to the wild-type ABCA1 (Figure S5H). Collectively, these findings delineate a non-proteolytic ubiquitination mechanism whereby Listerin catalyzes K63-linked polyubiquitination of ABCA1 at residues Lys1884 (located in flexible cytoplasmic loop adjacent to NBD2 domain) and Lys1957 (located in solvent-exposed region of the cytosolic NBD2 domain) to enhance cholesterol efflux capacity and mitigate foam cell pathogenesis.

Listerin deficiency aggravates the development of atherosclerosis in vivo

Then, we investigated the physiological role of Listerin in atherosclerosis. Listerin$^{fl/fl}$Lyz2^{Cre} mice were crossed with ApoE-/- mice to generate ApoE-/- Listerin$^{fl/fl}$Lyz2^{Cre} mice. ApoE-/-Listerin$^{fl/fl}$Lyz2^{Cre} mice and ApoE-/-Listerin$^{fl/fl}$ mice were fed a WD for 16 weeks, euthanized, and evaluated for atherosclerosis. The results show no significant difference in body weight (Figure 7A, Figure S6A), serum triglyceride, cholesterol, HDL, or LDL levels (Figure 7A, Figure S6A) between ApoE-/- Listerin$^{fl/fl}$ and ApoE-/-Listerin$^{fl/fl}$Lyz2^{Cre} mice. However, ApoE-/- Listerin$^{fl/fl}$ Lyz2^{Cre} mice exhibited many more lesions in the whole aorta and aortic root area than ApoE-/- Listerin$^{fl/fl}$ mice (Figure 7, B-D, Figure S6, B-D), Furthermore, the atherosclerotic lesion area and necrotic core area in the aortic root of ApoE-/- Listerin$^{fl/fl}$ Lyz2^{Cre} mice were significantly increased compared to ApoE-/- Listerin$^{fl/fl}$ mice (Figure 7E, Figure S6E). We then performed a more detailed analysis of aortic root components. When compared with ApoE-/-

Listerin$^{fl/fl}$ mice, morphological analyses of the cross-sectional lesions showed that the lipid accumulation and macrophage contents increased in ApoE-/- Listerin$^{fl/fl}$ Lyz2^{Cre} mice (Figure 7, F and G, Figure S6, F and G). We further examined ABCA1 expression levels in aortic lesions, and immunofluorescence of the aortic root and western blotting of whole aorta lysates showed that ABCA1 levels were significantly decreased in ApoE-/- Listerin$^{fl/fl}$Lyz2^{Cre} mice compared to that of ApoE-/- Listerin$^{fl/fl}$ mice (Figure 7, H and I, Figure S6, H and I). Taken together, these data show that Listerin deficiency in macrophages aggravates atherosclerosis development.

Listerin overexpression ameliorates the development of atherosclerosis in vivo

To further verify the atherosclerotic regulatory function of Listerin, we constructed a Listerin-overexpressing adenovirus with a macrophage-specific promoter Lyz2 (OE-Listerin adenovirus), and embryos the control (OE-CTR) and Listerin overexpressing virus into ApoE-/- mice. The mice were fed a WD for 16 weeks to evaluate the atherosclerosis. Immunofluorescence results showed that the expression of Listerin in plaques of OE-Listerin ApoE-/- mice was significantly increased compared with that of the control mice (OE-CTR ApoE-/-) (Figure S7A). In addition, there were no significant differences in body weight, cholesterol, triglycerides, HDL, and LDL between OE-CTR ApoE-/- mice and OE-Listerin ApoE-/- mice (Figure 8A). Assessment of the en face lesion area and Oil Red O staining of aortas revealed that the atherosclerotic lesion area in the whole aorta of OE-Listerin ApoE-/- mice was significantly reduced compared to that of OE-CTR ApoE-/- mice (Figure 8, B-D). Further, the H&E and Oil Red staining of aortic root lesions demonstrated that the lesion area, necrotic core area, and lipid deposition of OE-Listerin ApoE-/- mice was reduced compared to

the control group (Figure 8, E-F). The immunofluorescence staining results of aortic root lesions showed that, compared with the OE-CTR ApoE-/- mice, macrophage infiltration in OE-Listerin ApoE-/- mice were decreased (Figure 8G). Finally, we observed increased ABCA1 immunofluorescence staining in aortic root lesions of OE-Listerin ApoE-/- mice, which is consistent with the WB results of whole aorta lysates in these mice (Figure 8, H and I). Together, these data demonstrate that therapeutic overexpression of Listerin during atherosclerotic progression induced by WD can dramatically reduce aortic lesion areas by promoting ABCA1 expression.

Listerin regulates the progression of atherosclerosis through ABCA1

To further investigate the molecular mechanism by which Listerin regulates atherosclerosis progression and clarify the role of ABCA1 in this process, we conducted adenovirus-mediated overexpression of ABCA1 or its Listerin-targeted ubiquitination-site mutant (K1884R/K1957R) in macrophage-specific Listerin-knockout mice to determine whether ABCA1 reconstitution could counteract the pro-atherogenic effects of Listerin deficiency. In a WD-induced atherosclerosis model, no significant differences in body weight, cholesterol, triglycerides, HDL, or LDL levels were observed among $ApoE^{-/-}Listerin^{fl/fl}$, $ApoE^{-/-}Listerin^{fl/fl}Lyz2^{Cre}$, $ApoE^{-/-}Listerin^{fl/fl}Lyz2^{Cre}$+ABCA1, or $ApoE^{-/-}Listerin^{fl/fl}Lyz2^{Cre}$+ABCA1 (mut) groups (Figure S9A). However, en face aortic lesion analysis (Figure S9B) and Oil Red O staining (Figure S9C) demonstrated that Listerin knockout exacerbated AS progression, whereas overexpression of ABCA1 or its ubiquitination-site mutant reversed the pro-atherogenic effects caused by Listerin deficiency, restoring plaque burden to control levels. Western blot further

confirmed reduced ABCA1 protein expression in Listerin-KO plaques, which was rescued by overexpression of either wild-type ABCA1 or its ubiquitination-defective mutant (Figure S9D).

Finally, we generated macrophage-specific Listerin overexpression adenovirus (OE-Listerin) and ABCA1 knockdown adeno-associated virus (shABCA1-AAV). These viruses, alongside control viruses, were delivered into ApoE-/- mice fed a WD to establish an atherosclerosis model. Immunofluorescence confirmed significant downregulation of ABCA1 in atherosclerosis plaques and macrophages following shABCA1-AAV administration (Fig. S8A). No differences in body weight, cholesterol, triglycerides, HDL, or LDL levels were observed among the OE-Ctrl ApoE-/-, OE-Listerin ApoE-/-, and shABCA1+OE-Listerin ApoE-/- groups (Figure S9E). Evaluation of en face aortic lesion area (Figure S9F) and Oil Red O staining (Figure S9G) revealed reduced plaque area in Listerin-overexpressing macrophages (OE-Listerin ApoE-/- mice), and abrogation of Listerin's protective effect upon concurrent ABCA1 knockdown (shABCA1+OE-Listerin ApoE-/- mice). Finally, western blot of ABCA1 revealed increased ABCA1 in OE-Listerin lesions, and restoration of ABCA1 to control levels in shABCA1+OE-Listerin mice (Figure S9H). These data collectively demonstrate that therapeutic Listerin overexpression attenuates aortic lesion area in WD-induced atherosclerosis by ubiquitinating ABCA1 at lysine residues K1884 and K1957 to stabilize and upregulate ABCA1 expression, thereby establishing ABCA1 as the critical mediator of Listerin's atheroprotective effects.

DISCUSSION

ABCA1 is a pivotal cholesterol transporter on macrophages that mediates cholesterol efflux to extracellular acceptors (ApoA1), and accumulating evidence has shown that macrophage ABCA1 alone plays an important role in atherogenesis. Macrophage ABCA1 degradation leads to lipid deposition and foam formation in macrophages, promoting the development of atherosclerosis (46-50). Targeting macrophage ABCA1 emerges as a viable strategy for attenuating atherosclerotic progression. In addition, it has been reported that advanced glycation end-product (AGE)-albumin diminishes ABCA1 by accelerating its ubiquitination and degradation through the proteasomal and lysosomal systems (37). Forced expression of COP9 signalosome subunit 3 (CSN3) inhibits thrombin-induced ABCA1 ubiquitination and degradation (47). Cell cholesterol loading also inhibits the ubiquitination and proteasomal degradation of ABCA1 and ABCG1 (51). Aside from protein degradation, ubiquitination is also closely related to protein stability or trafficking of ABCA1 (22, 52-54), which plays an important role in atherosclerosis. In the human hepatoma cell line HepG2, but not in PMs, the long form of Pim1 (Pim1L) interacts with cell surface-resident ABCA1 (csABCA1), thereby protecting it from ubiquitination and subsequent lysosomal degradation via its phosphorylation function (54). In another study, the authors found that csABCA1 degradation is inhibited by overexpression of a dominant-negative form of ubiquitin. Moreover, disruption of the ESCRT pathway, a dominant mechanism for ubiquitination-mediated lysosomal degradation, significantly delays the degradation of cell surface-resident ABCA1(22).

The above studies showed that, with the help of ubiquitination modifications, ABCA1 becomes unstable and is easily degraded through the proteasome or lysosome pathway (37),

and the ESCRT pathway plays an important role in the stability and trafficking of ABCA1(22). However, some key scientific questions regarding ABCA1 ubiquitin modification remain unanswered. First, an E3 ligase that directly binds to ABCA1 has not yet been identified. Second, many types of protein ubiquitination exist, and different types of ubiquitin modifications have different effects on protein function. For example, K48-linked polyubiquitination usually regulates protein degradation, and K63-linked polyubiquitination might be related to protein translocation and signaling activation (55). To date, no detailed studies have been performed on the different types of ubiquitin modifications of ABCA1. Third, the ESCRT-lysosome is an important pathway that regulates ABCA1 protein stability, but the mechanism of ubiquitination is still unclear. In our study, we found that Listerin was essential for the degradation of cell surface-resident ABCA1 through the ESCRT system, because ABCA1 protein levels were restored by either HRS-specific siRNA or the ESCRT inhibitor DBeQ in Listerin-deficient PMs. Furthermore, our research shows that Listerin, acting as an E3 ubiquitin ligase, bound ABCA1 and promoted K63-linked polyubiquitination of ABCA1 at lysine sites K1884 and K1957, which inhibited its translocation from the cytomembrane and degradation through the ESCRT-lysosome pathway.

Several studies have demonstrated that LTN1 (a yeast homolog of Listerin), is a component of the RQC complex, especially in yeast and bacteria, which mediates the ubiquitination and extraction of incompletely synthesized nascent chains for proteasomal degradation with its cofactor Rqc2 (NEMF in mammals) (42-44). Unlike Rqc2/NEMF, the core component of the RQC system, recent studies have shown that Listerin may play other roles independent of the RQC system in more complex mammalian cells (48, 56-58), For instance, Listerin negatively

regulates the cGAS-mediated immune response by facilitating the degradation of the cGAS protein via the ESCRT pathway (48). Another study reports that Listerin also negatively modulates RLR-mediated antiviral innate immunity against RNA viruses through the ESCRT pathway (57). While the cGAS-STING signaling pathway has been well-documented in mediating inflammatory responses during atherosclerosis progression (59), emerging evidence suggests potential cross-talk between Listerin and cGAS in viral infection contexts. Our experiments revealed no detectable changes in cGAS expression within atherosclerotic plaques of macrophage-specific Listerin-knockout or overexpression mice compared to control mice (data not shown). This observation suggests that, unlike its role in acute infectious diseases, Listerin may regulate alternative targets beyond the cGAS-STING axis in chronic pathologies like atherosclerosis. These findings highlight that Listerin engages distinct molecular targets and modulates divergent biological processes depending on cellular context and pathological milieu, thereby revealing a unique mechanistic framework in atherosclerosis pathogenesis. Our study found that Listerin targets ABCA1 for K63-linked polyubiquitination independent of the RQC system, and also further supported the idea that Listerin might play important roles in mammals.

As mentioned above, E3 ubiquitin ligase LTN1 (a yeast homolog of Listerin) has attracted increasing attention, focusing on yeast and *in vitro* translation systems (42-44). Exploring the role of Listerin in mammalian physiology and disease is necessary. In our study, Listerin conditional knockout mice were generated, and we found that ApoE-/- Listerin$^{fl/fl}$ Lyz2^{Cre} mice showed more severe plaque progression than ApoE-/- Listerin$^{fl/fl}$ mice. Conversely, macrophage-specific overexpression of Listerin attenuated plaque formation compared to

control mice. Critically, Listerin's regulation of atherosclerotic plaques is dependent on ABCA1. Furthermore, no significant differences in body weight or serum lipid profiles were observed between the groups. The potential reason for unchanged murine lipid profiles following Listerin intervention is that unlike hepatocytes-where cholesterol metabolism directly regulates systemic serum lipid levels-sparsely distributed macrophages predominantly influence local vascular cholesterol accumulation. These data demonstrate the physiological phenomenon in mice that loss of Listerin in macrophages aggravates atherosclerosis progression. It has been reported that mutations in Listerin cause neurodegeneration in mice (60), but the mechanism details were not revealed. ApoE lipidation, which was controlled by the activity of the ABCA1, was reported to play a central role in β-amyloid (Aβ) accumulation and Alzheimer's disease (AD) pathology. Enhancing ABCA1 recycling to the membrane could restore ABCA1 activity and enhance β-amyloid (Aβ) degradation (52). In our study, we found that Listerin could combine with ABCA1 and promote K63-linked polyubiquitination of ABCA1, which inhibited its translocation from the cytomembrane and its degradation. Our data might partly explain why Listerin mutations aggravate neurodegeneration in mice.

In summary, our study demonstrates that the macrophage Listerin has an important effect on the pathogenesis of atherosclerosis, differently from yeast and bacteria, and reveals another regulatory mechanism of ABCA1. Listerin catalyzed K63-linked polyubiquitination of ABCA1 at lysine sites K1884 and K1957 and inhibited its degradation through the ESCRT-lysosome pathway, which further promoted the cholesterol efflux of macrophages, inhibited foam cell formation, and ameliorated atherosclerosis development. Since macrophages play a key role in atherosclerosis progression, macrophage-mediated pro-atherosclerotic processes are important

targets for developing diagnostic imaging and therapies for atherosclerosis (3). Nanotherapy targeting macrophage Listerin may be a meaningful therapeutic strategy for ameliorating atherosclerosis by activating the macrophage cholesterol efflux receptor ABCA1.

MATERIALS AND METHODS

All data supporting the findings of this study can be made available to other researchers for reproducing the results or replicating the procedures. The detailed materials and methods are provided in the Supplemental Materials.

Sex as a biological variant.

Our study examined both males and females in mouse experimental models, human biospecimen studies and human peripheral blood mononuclear cells, and similar findings are reported for both sexes; therefore, sex was not considered as a biological variable.

Animals

Listerin-deficient mice were generated by Beijing Biocytogen (USA) using the CRISPR/Cas9 system and genotyping of mice was performed using the primers Forward5′GGAGTTACAGCTGGGAGTTGTCGTG3′ and Reverse5′GCTCAGCAATATCACAACGCTGCAT -3′. The mice were crossed with $Lyz2^{cre}$ mice (B6.129P2-Lyz2tm1(cre)Ifo/J, Jackson Laboratory) to obtain $Listerin^{fl/fl}Lyz2^{cre}$ mice. These mice were then backcrossed onto the C57BL/6 background (GemPharmatech Co., Ltd #N000013). Furthermore, $Listerin^{fl/fl}Lyz2^{cre}$ mice were crossed with ApoE-/-(B6.129P2-Apoetm1Unc/J, Jackson Laboratory) mice to obtain ApoE-/- $Listerin^{fl/fl}Lyz2^{cre}$ mice, and these mice were also backcrossed onto the C57BL/6 background (GemPharmatech Co., Ltd #N000013). To generate an atherosclerosis animal model, mice were fed a Western diet (WD)

for 16 weeks. All mice exhibited no difference in phenotypes and both male and female mice were used. Based on our preliminary experiment results, we set the significance level (α) at 0.05, and power (1-β) at 80% to confirm the sample size, and 8–10 animals were analyzed in each group. The animals were grouped randomly and blindly. In the final analysis, animals that were sick or died before euthanasia were not included.

Human coronary artery samples

Human coronary atherosclerotic plaques were obtained from autopsy specimens of 6 male body donors with coronary heart disease after sudden coronary death, and the bodies were provided by the Red Cross Society of Shandong Province, China. Baseline characteristics of the human specimens used in the study are listed in Supplementary Table S3. The coronary arteries were embedded with optimal cutting temperature compound (OCT, Sakura, Japan) and cut into 7-μm-thick cross sections for histopathological staining.

Cell culture

HEK293T cell, Hela cell, THP-1 and RAW264.7 macrophages were obtained from KeyGene BioTech (China). Primary peritoneal macrophages were extracted from Listerin$^{fl/fl}$Lyz2^{cre} mice and their control littermates or C57BL/6J wild-type mice after being injected intraperitoneally with 1 ml of 6% sterile starch, and all of these cells were cultured in DMEM containing 10% FBS (Fetal bovine serum) and 1% penicillin-streptomycin at 37 ℃.

Analysis of atherosclerotic plaque

After 16 weeks of being fed a WD, the mice fasted for 12 h, and mice were euthanized using a single dose of pentobarbital (150 mg/kg, i.p.). Blood was drawn from the left ventricle and perfused with cold saline, and the heart and whole aorta were removed and fixed with 4%

paraformaldehyde. For analysis of en face aorta, the paraformaldehyde was washed away with saline, and the surrounding adipose tissue was removed and examined under a microscope, and the aorta was cut longitudinally for Oil Red O staining. For aortic root atherosclerotic lesions, the base of the heart and the root of the ascending aorta were dissected, embedded with OCT, and we collected sequential cross-sections at 7-μm distance per section from the origin of the aortic valves to the ascending aorta. The frozen sections were stained with hematoxylin-eosin (H&E), Oil red O, and immunofluorescent staining, complying with the manufacturer's instructions. Then, the stained slides were observed under a microscope. Researchers were blinded to the mouse genotype for the measurement of atherosclerotic plaque.

Statistics analysis

For immunoblots, protein band intensities were quantified using ImageJ software (version 1.52a, National Institutes of Health, USA) and normalized to corresponding GAPDH levels. All data are expressed as mean ± standard deviation (SD). Statistical analyses were performed using GraphPad Prism 8 (GraphPad Software, San Diego, CA), with each experiment independently repeated at least three times. Normally distributed data were analyzed by unpaired two-tailed Student's t-tests, while non-normally distributed data were assessed using the Mann-Whitney U test. For one-variable comparisons across multiple groups, one-way ANOVA with Dunnett's post-hoc test was applied. Multivariate comparisons were conducted through two-way ANOVA followed by Sidak's multiple comparisons test. Non-Gaussian distributed single-variable datasets were subjected to Kruskal-Wallis testing with Dunnett's post-hoc analysis for intergroup comparisons. Values of $P < 0.05$ were considered significant.

Study approval

All experiments using human being were reviewed and approved by the Ethical Committee of Qilu Hospital of Shandong University (**No. KYLL 2022(ZM)-427)**, and written, informed consent was obtained from all participants. All the experiments on mice were conducted in accordance with the National Institutes of Health (NIH) Guide for the Care and Use of Laboratory Animals and approved by the Ethical Committee of Qilu Hospital of Shandong University **(No. KYLL 2022(ZM)-427).**

Data availability

RNA sequencing data are stored in the NCBI SRA database under accession number PRJNA1269750. Proteomics data are stored in ProteomeXchange with accession numbers PXD064532 and PXD064538.

Author contributions:

M.Z, C.Z. and C.G. conceived the study, directed the research, and supervised all experimental work. L.C., J.Z., L.Y. performed most experiments, collected all the data, participated in result analysis, visualized data in publication-ready figures, and wrote the manuscript. W.Y., W.Q., R.R., Y.L., Y.H. and Y.C. contributed to animal experiments and conducted laser confocal immunofluorescence detection. Q.L., X.W., W.S., Y.Z. participated in project discussions and data analysis. B.L performed clinical blood sample collection. Z.Z obtained atherosclerotic tissue specimens. Funding acquisition was the responsibility of C.Z. and M.Z. All authors have read and approved the article.

Acknowledgments

We thank Dr. Zhengguo Zhang (Qilu Hospital of Shandong University, China) for providing the tissue samples.

References and Notes

1. Writing Group M, et al. Heart Disease and Stroke Statistics-2016 Update: A Report From the American Heart Association. Circulation. 2016;133(4):e38-360.
2. Libby P. Inflammation in atherosclerosis. Arterioscler Thromb Vasc Biol. 2012;32(9):2045-51.
3. Chen W, et al. Macrophage-targeted nanomedicine for the diagnosis and treatment of atherosclerosis. Nat Rev Cardiol. 2022;19(4):228-49.
4. Cao Y, et al. Update on therapeutic neovascularization. Cardiovasc Res. 2005;65(3):639-48.
5. Moore KJ, et al. Macrophages in atherosclerosis: a dynamic balance. Nat Rev Immunol. 2013;13(10):709-21.
6. Liu M, et al. Macrophage K63-Linked Ubiquitination of YAP Promotes Its Nuclear Localization and Exacerbates Atherosclerosis. Cell Rep. 2020;32(5):107990.
7. Brakenhielm E, et al. Lymphatics in the broken heart. J Clin Invest. 2021;131(20):e153448.
8. Kruth HS. Sequestration of aggregated low-density lipoproteins by macrophages. Curr Opin Lipidol. 2002;13(5):483-8.
9. Glass CK, Witztum JL. Atherosclerosis. the road ahead. Cell. 2001;104(4):503-16.
10. Hansson GK, Hermansson A. The immune system in atherosclerosis. Nat Immunol. 2011;12(3):204-12.
11. Guo L, et al. CD163+ macrophages promote angiogenesis and vascular permeability accompanied by inflammation in atherosclerosis. J Clin Invest. 2018;128(3):1106-24.
12. Rosenson RS, et al. Cholesterol efflux and atheroprotection: advancing the concept of reverse cholesterol transport. Circulation. 2012;125(15):1905-19.
13. Neufeld EB, et al. Cellular localization and trafficking of the human ABCA1 transporter. J Biol Chem. 2001;276(29):27584-90.
14. Singaraja RR, et al. Palmitoylation of ATP-binding cassette transporter A1 is essential for its trafficking and function. Circ Res. 2009;105(2):138-47.
15. Quazi F, Molday RS. Differential phospholipid substrates and directional transport by ATP-binding cassette proteins ABCA1, ABCA7, and ABCA4 and disease-causing mutants. J Biol Chem. 2013;288(48):34414-26.
16. Rosenson RS, et al. Dysfunctional HDL and atherosclerotic cardiovascular disease. Nat Rev Cardiol. 2016;13(1):48-60.
17. Haas MJ, Mooradian AD. Potential Therapeutic Agents That Target ATP Binding Cassette A1 (ABCA1) Gene Expression. Drugs. 2022;82(10):1055-75.
18. Westerterp M, et al. ATP-binding cassette transporters, atherosclerosis, and inflammation. Circ Res. 2014;114(1):157-70.
19. Han YH, et al. Enterically derived high-density lipoprotein restrains liver injury through the portal vein. Science. 2021;373(6553).
20. Feig JE. Regression of atherosclerosis: insights from animal and clinical studies. Ann Glob Health. 2014;80(1):13-23.
21. Tall AR, et al. HDL, ABC transporters, and cholesterol efflux: implications for the treatment of atherosclerosis. Cell Metab. 2008;7(5):365-75.
22. Mizuno T, et al. Ubiquitination is associated with lysosomal degradation of cell surface-resident ATP-binding cassette transporter A1 (ABCA1) through the endosomal sorting complex required for transport (ESCRT) pathway. Hepatology. 2011;54(2):631-43.
23. Zhou ZX, et al. The Role of Ubiquitin E3 Ligase in Atherosclerosis. Curr Med Chem. 2021;28(1):152-

68.
24. Wang B, et al. Disruption of USP9X in macrophages promotes foam cell formation and atherosclerosis. J Clin Invest. 2022;132(10):e154217.
25. Liu Z, et al. Macrophage Liver Kinase B1 Inhibits Foam Cell Formation and Atherosclerosis. Circ Res. 2017;121(9):1047-57.
26. Luo Y, et al. Macrophagic CD146 promotes foam cell formation and retention during atherosclerosis. Cell Res. 2017;27(3):352-72.
27. Li AC, Glass CK. The macrophage foam cell as a target for therapeutic intervention. Nat Med. 2002;8(11):1235-42.
28. Chistiakov DA, et al. Mechanisms of foam cell formation in atherosclerosis. J Mol Med (Berl). 2017;95(11):1153-65.
29. Wang D, et al. Targeting Foam Cell Formation in Atherosclerosis: Therapeutic Potential of Natural Products. Pharmacol Rev. 2019;71(4):596-670.
30. Ouimet M, et al. HDL and Reverse Cholesterol Transport. Circ Res. 2019;124(10):1505-18.
31. Frambach S, et al. Brothers in Arms: ABCA1- and ABCG1-Mediated Cholesterol Efflux as Promising Targets in Cardiovascular Disease Treatment. Pharmacol Rev. 2020;72(1):152-90.
32. Cedo L, et al. LDL Receptor Regulates the Reverse Transport of Macrophage-Derived Unesterified Cholesterol via Concerted Action of the HDL-LDL Axis: Insight From Mouse Models. Circ Res. 2020;127(6):778-92.
33. Yu XH, et al. Cholesterol transport system: An integrated cholesterol transport model involved in atherosclerosis. Prog Lipid Res. 2019;73:65-91.
34. Mineo C. Lipoprotein receptor signalling in atherosclerosis. Cardiovasc Res. 2020;116(7):1254-74.
35. Miyazaki T, et al. Calpain and atherosclerosis. J Atheroscler Thromb. 2013;20(3):228-37.
36. Yokoyama S, et al. Calpain-mediated ABCA1 degradation: post-translational regulation of ABCA1 for HDL biogenesis. Biochim Biophys Acta. 2012;1821(3):547-51.
37. Iborra RT, et al. AGE-albumin enhances ABCA1 degradation by ubiquitin-proteasome and lysosomal pathways in macrophages. J Diabetes Complications. 2018;32(1):1-10.
38. Raiborg C, Stenmark H. The ESCRT machinery in endosomal sorting of ubiquitylated membrane proteins. Nature. 2009;458(7237):445-52.
39. Zhang W, et al. A conserved ubiquitin- and ESCRT-dependent pathway internalizes human lysosomal membrane proteins for degradation. PLoS Biol. 2021;19(7):e3001361.
40. Hurley JH, Hanson PI. Membrane budding and scission by the ESCRT machinery: it's all in the neck. Nat Rev Mol Cell Biol. 2010;11(8):556-66.
41. Feng X, et al. Hypoxia-induced acetylation of PAK1 enhances autophagy and promotes brain tumorigenesis via phosphorylating ATG5. Autophagy. 2021;17(3):723-42.
42. Brandman O, Hegde RS. Ribosome-associated protein quality control. Nat Struct Mol Biol. 2016;23(1):7-15.
43. Bengtson MH, Joazeiro CA. Role of a ribosome-associated E3 ubiquitin ligase in protein quality control. Nature. 2010;467(7314):470-3.
44. Joazeiro CAP. Mechanisms and functions of ribosome-associated protein quality control. Nat Rev Mol Cell Biol. 2019;20(6):368-83.
45. Lyumkis D, et al. Structural basis for translational surveillance by the large ribosomal subunit-associated protein quality control complex. Proc Natl Acad Sci U S A. 2014;111(45):15981-6.
46. Westerterp M, et al. Cholesterol Efflux Pathways Suppress Inflammasome Activation, NETosis, and

Atherogenesis. Circulation. 2018;138(9):898-912.
47. Boro M, et al. Thrombin-Par1 signaling axis disrupts COP9 signalosome subunit 3-mediated ABCA1 stabilization in inducing foam cell formation and atherogenesis. Cell Death Differ. 2021;28(2):780-98.
48. Qin F, et al. Listerin promotes cGAS protein degradation through the ESCRT pathway to negatively regulate cGAS-mediated immune response. Proc Natl Acad Sci U S A. 2023;120(52):e2308853120.
49. van Eck M, et al. Leukocyte ABCA1 controls susceptibility to atherosclerosis and macrophage recruitment into tissues. Proc Natl Acad Sci U S A. 2002;99(9):6298-303.
50. Aiello RJ, et al. Increased atherosclerosis in hyperlipidemic mice with inactivation of ABCA1 in macrophages. Arterioscler Thromb Vasc Biol. 2002;22(4):630-7.
51. Hsieh V, et al. Cellular cholesterol regulates ubiquitination and degradation of the cholesterol export proteins ABCA1 and ABCG1. J Biol Chem. 2014;289(11):7524-36.
52. Rawat V, et al. ApoE4 Alters ABCA1 Membrane Trafficking in Astrocytes. J Neurosci. 2019;39(48):9611-22.
53. Azuma Y, et al. The COP9 signalosome controls ubiquitinylation of ABCA1. Biochem Biophys Res Commun. 2009;382(1):145-8.
54. Katsube A, et al. Pim-1L Protects Cell Surface-Resident ABCA1 From Lysosomal Degradation in Hepatocytes and Thereby Regulates Plasma High-Density Lipoprotein Level. Arterioscler Thromb Vasc Biol. 2016;36(12):2304-14.
55. Swatek KN, Komander D. Ubiquitin modifications. Cell Res. 2016;26(4):399-422.
56. Zuzow N, et al. Mapping the mammalian ribosome quality control complex interactome using proximity labeling approaches. Mol Biol Cell. 2018;29(10):1258-69.
57. Qin F, et al. LTN1 promotes RLR degradation to inhibit immune response to RNA virus through the ESCRT pathway. Autophagy. 2024;20(6):1270-85.
58. Lv L, et al. NEMF-mediated Listerin-independent mitochondrial translational surveillance by E3 ligase Pirh2 and mitochondrial protease ClpXP. Cell Rep. 2024;43(3):113860.
59. Pham PT, et al. STING, a cytosolic DNA sensor, plays a critical role in atherogenesis: a link between innate immunity and chronic inflammation caused by lifestyle-related diseases. Eur Heart J. 2021;42(42):4336-48.
60. Chu J, et al. A mouse forward genetics screen identifies LISTERIN as an E3 ubiquitin ligase involved in neurodegeneration. Proc Natl Acad Sci U S A. 2009;106(7):2097-103.

Supplementary Materials

Supplemental Methods

Figures S1–S9 Tables S1–S4

Funding

This work was supported by grants of the National Natural Science Foundation of China (No. 82270487, 81920108003, 82241203, 82200502, 82400492 and 82200507); the Postdoctoral Science Foundation of China and Shandong Province (2024M751833, 2023TQ0196,

2023M742127, SDCX-ZG-202400012); the National Key Research and Development Program of China (2021YFF0501403); the Shandong Provincial Natural Science Foundation (ZR2023JQ030, 2021ZLGX02, 2021ZDSYS05); the Program of Introducing Talents of Discipline to Universities (BP0719033), Non-profit Central Research Institute Fund of Chinese Academy of Medical Sciences (2023-PT320-06); the Taishan Scholars Program of Shandong Province (tsqn202408348, Zhang M and Zhang C); Shandong Province Postdoctoral Innovation Talent Program (SDBX202302025).

Competing interests

The authors declare no competing interests.

Figures

Figure1

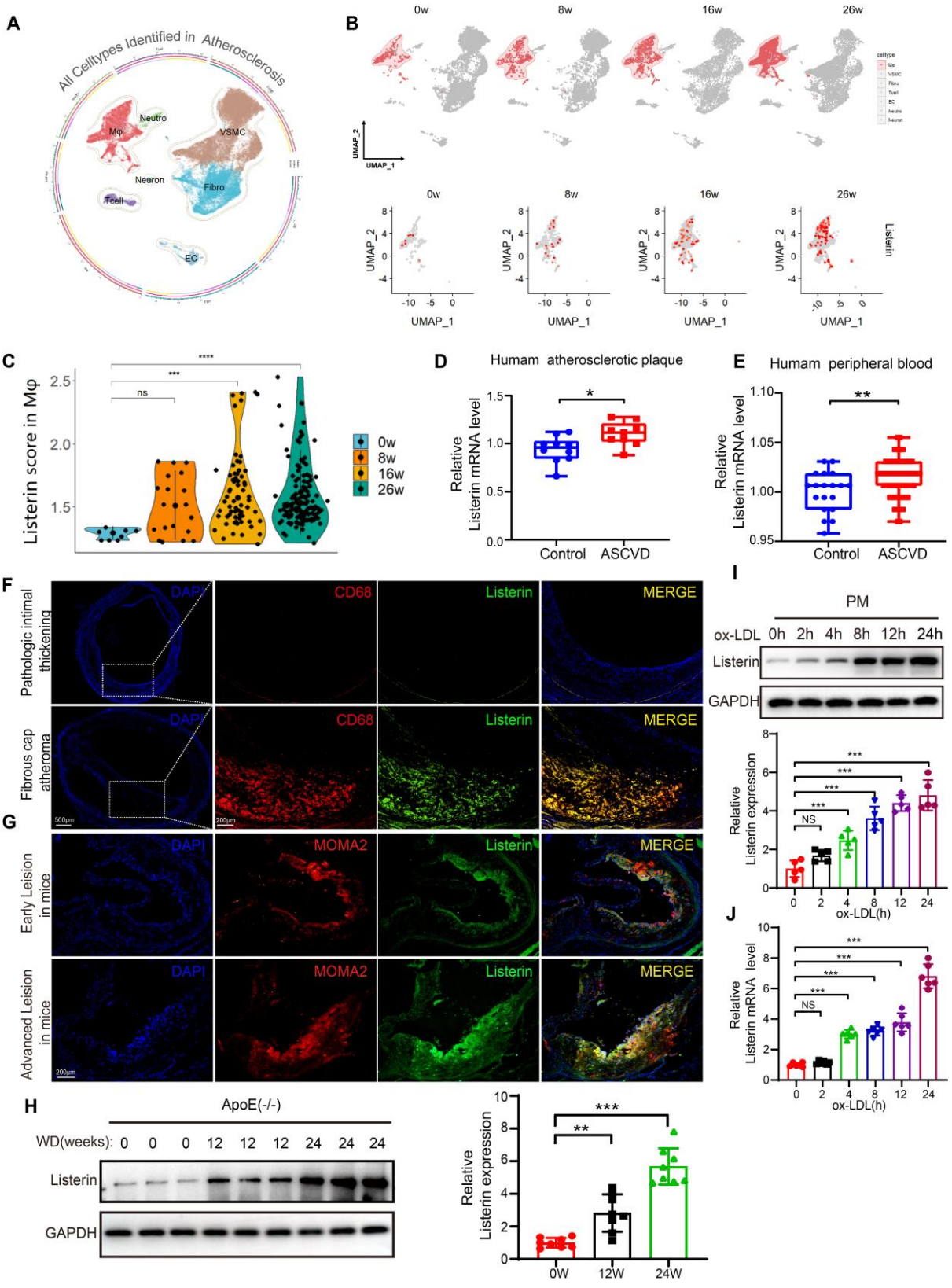

Figure1. Listerin expression increases in human and mouse atherosclerotic plaque tissues

(A) All celltypes identified in atherosclerotic plaque samples (n=8) and 28687 cells were obtained after filted with seven cell types mapped on. **(B)** The proportion of macrophages was specifically increased with the progression of plaques. **(C)** The number and the expression level of Listerin in macrophages of atherosclerosis in different timepoints. **(D)** Listerin expression in human atherosclerotic plaque was obtained from Gene Expression Omnibus databases (GSE57691). **(E)** Listerin expression in human peripheral blood mononuclear cells was obtained from Gene Expression Omnibus databases (GSE23749). **(F)** Immunofluorescence staining of Listerin (green particles) and CD68 (red particles) in pathological intimal thickening and fibroatheroma in human coronary artery atherosclerotic plaques. n=5 per group. Scale bar=500μm and 200μm. **(G)** Immunofluorescence staining of Listerin (green particles) and MOMA2 (red particles) in early lesions (WD for 8 weeks) and advanced lesions (WD for 24 weeks) in mice (male). n = 8 per group. Scale bar=200μm. **(H)** Immunoblot analysis of Listerin expression in the whole-aorta lysates of ApoE-/- mice fed a Western diet (WD) for 0,12,24 weeks. n = 8 per group. **(I)** Immunoblot analysis of Listerin expression in PMs after oxLDL (50μg/mL) treatment. n = 5 per group. **(J)** Quantitative RT-PCR analysis of Listerin mRNA levels in PMs after oxLDL (50μg/mL) treatment at the indicated time. n = 6 per group. Data were presented as mean ± SD, the Shapiro–Wilk method was used to test the normal distributions and statistical analysis was performed by Student's *t*-test for D and E. Mann-Whitney Test was used for C. One-way ANOVA with Dunnett post hoc test was used for H, I and J. For multiple-group comparisons, the adjusted P-values are provided, NS (not significant) $P > 0.05$, $*P < 0.05$, $**P < 0.01$, and $***P < 0.001$. Each experiment was obtained at least three

times independently.

Figure2

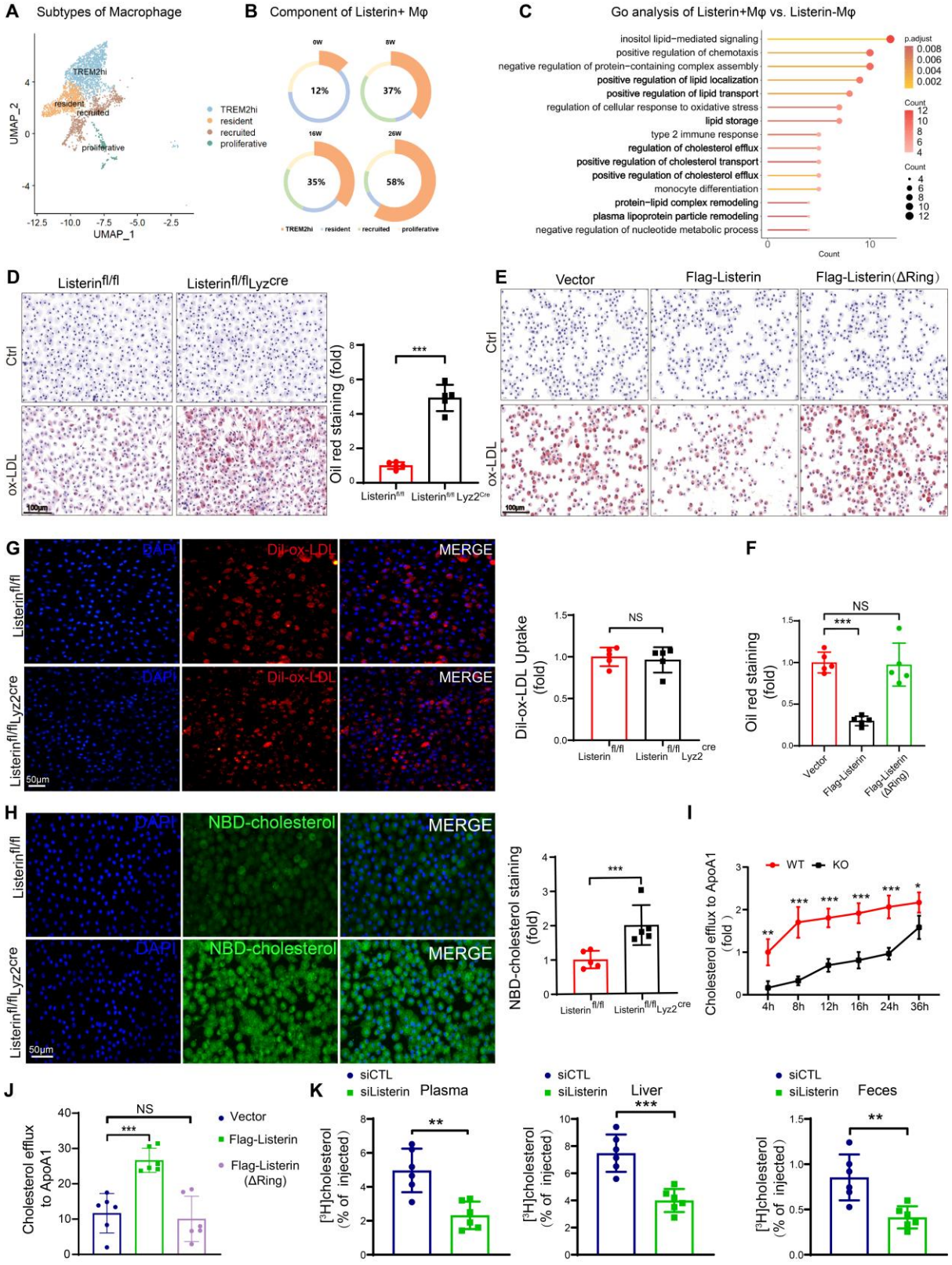

Figure2. Macrophage Listerin knockout inhibits cholesterol efflux and aggravates foam cell

formation **(A)** The subtypes of macrophages were identified into four different subpopulations. **(B)** The component of Listerin + macrophages among the four subtypes of macrophages as the atherosclerosis progressed. **(C)** GO pathways analysis of DEGs (differential expressed genes) in Listerin+ macrophages. **(D)** Oil red O staining images and quantitation of PMs from Listerin$^{fl/fl}$ and Listerin$^{fl/fl}$Lyz2^{cre} mice after incubation with or without oxLDL (50 μg/mL) for 24 hours. n=5 per group. Scale bar=100μm. **(E)** Oil red O staining images and quantitation **(F)** of PMs incubated with or without oxLDL (50 μg/mL) for 24 hours after adenovirus-mediated overexpression of Flag-Listerin and Flag–Listerin-ΔRing. n=5 per group. Scale bar=100μm. **(G)** Immunofluorescence images and quantitation of PMs from Listerin$^{fl/fl}$ and Listerin$^{fl/fl}$Lyz2^{cre} mice treated with Dil-oxLDL (40μg/mL) at 37°C for 4 h. n=5 per group. Scale bar=100μm. **(H)** Immunofluorescence images and quantitation of PMs pre-loaded with the NBD-cholesterol and then incubation with ApoA1 for 4 h. n=5 per group. Scale bar=50μm. **(I)** Time-course of ApoA1-mediated cholesterol efflux assay of PMs from Listerin$^{fl/fl}$ and Listerin$^{fl/fl}$Lyz2^{cre} mice. n=3 per group. **(J)** ApoA1-mediated cholesterol efflux assay of PMs infected with indicated adenovirus. n=6 per group. **(K)** The percent appearance of [3^{H}] cholesterol in plasma, liver, and feces 48 h after transplanting cholesterol-loaded RAW 264.7 macrophages transfected with either NC or Listerin-siRNA, n=6 per group. Data were presented as mean ± SD and the Shapiro–Wilk method was used to test the normal distributions. Statistical analysis was performed by Student's *t*-test for D, G and K. Mann-Whitney Test was used for H. Two-way ANOVA followed by Sidak post hoc test was used for I. One-way ANOVA with Dunnett post hoc test was used for F and G. For multiple-group comparisons, the adjusted P-values are provided, NS (not significant) $P > 0.05$, *$P < 0.05$, **$P < 0.01$, ***$P <$

0.001.

Figure3

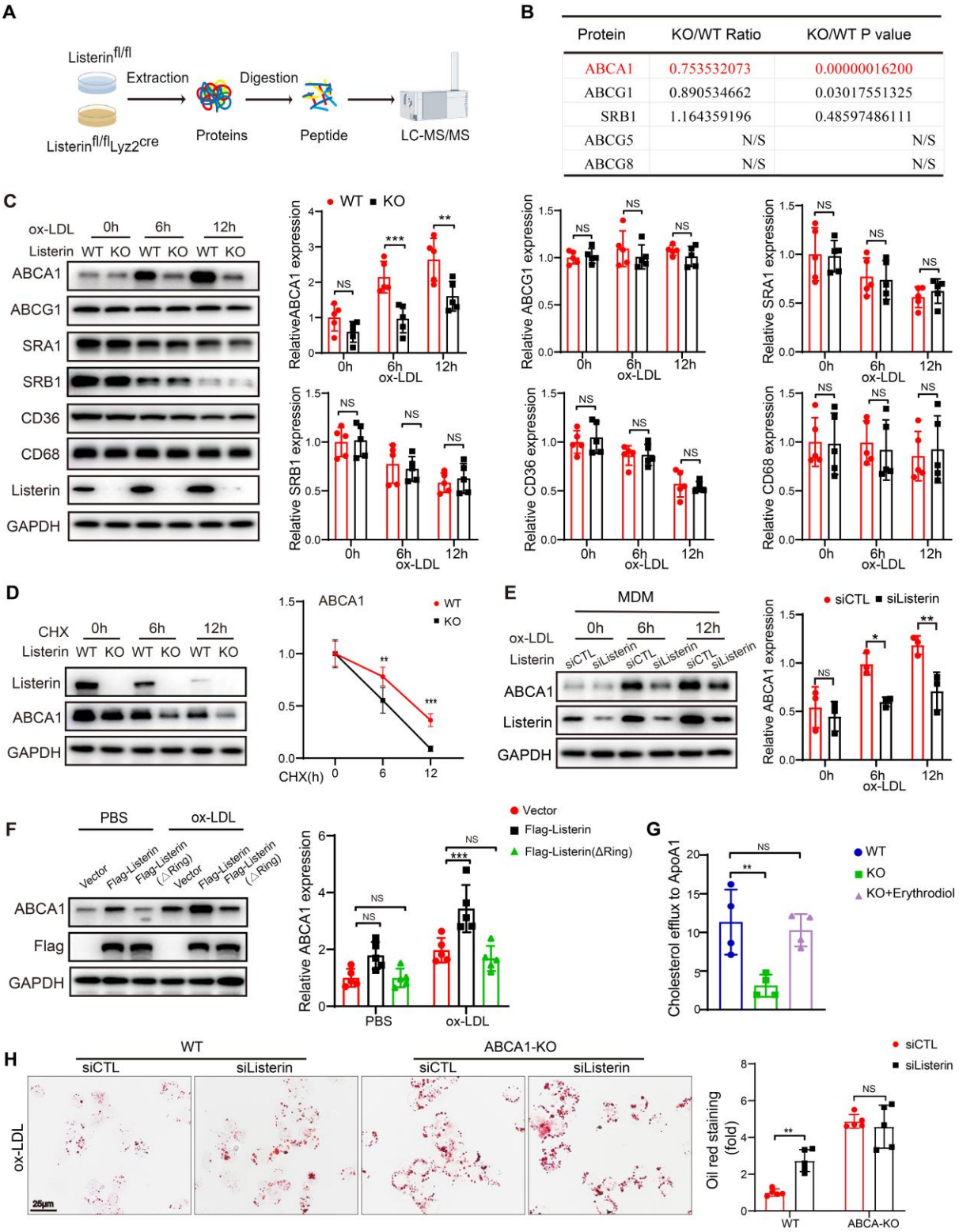

Figure3. Listerin knockout promotes lipid accumulation and foam cell formation through

downregulating ABCA1 **(A)** Diagram of 4D-FastDIA-based quantitative proteomic of PMs isolated from Listerin$^{fl/fl}$ and Listerin$^{fl/fl}$Lyz2^{cre}. **(B)** 4D-FastDIA-based quantitative proteomic of cholesterol efflux related receptors expression in macrophages after Listerin knockout. **(C)** Immunoblot analysis of indicated proteins in Listerin$^{fl/fl}$ and Listerin$^{fl/fl}$Lyz2^{cre} PMs after oxLDL treatment. n=5 per group. (**D)** Immunoblot and quantitative analysis of ABCA1 expression in PMs obtained from Listerin$^{fl/fl}$ and Listerin$^{fl/fl}$Lyz2^{cre} mice, the cells were treated with oxLDL for 12h, then treated with cycloheximide (CHX, 50μg/ml) at various times. **(E)** Immunoblot analysis of ABCA1 expression in MDM [derived from PBMC induced by M-CSF (50ng/mL) for 7 days] after Listerin knockdown. n=3 per group. **(F)** Immunoblot analysis of ABCA1 expression after adenovirus-mediated overexpression of Flag-Listerin or Flag-Listerin(ΔRing) in PMs. n=5 per group. **(G)** ApoA1-mediated cholesterol efflux assay of PMs isolated from Listerin$^{fl/fl}$ and Listerin$^{fl/fl}$Lyz2^{cre} mice, PMs pre-incubated with or without ABCA1 agonist Erythrodiol. n=4 per group. **(H)** Oil red O staining images and quantitation of WT and ABCA1-KO THP-1 cells transfected with siCTL or siListerin. n=5 per group. Scale bar=25μm. Data were presented as mean ± SD and the Shapiro–Wilk method was used to test the normal distributions. Two-way ANOVA followed by Tukey post hoc test was used for F. The C, D, E and H were Two-way ANOVA followed by Sidak post hoc test. One-way ANOVA with Dunnett post hoc test was used for G. For multiple-group comparisons, the adjusted P-values are provided, NS (not significant) $P > 0.05$, $^{**}P < 0.01$ and $^{***}P < 0.001$.

Figure4

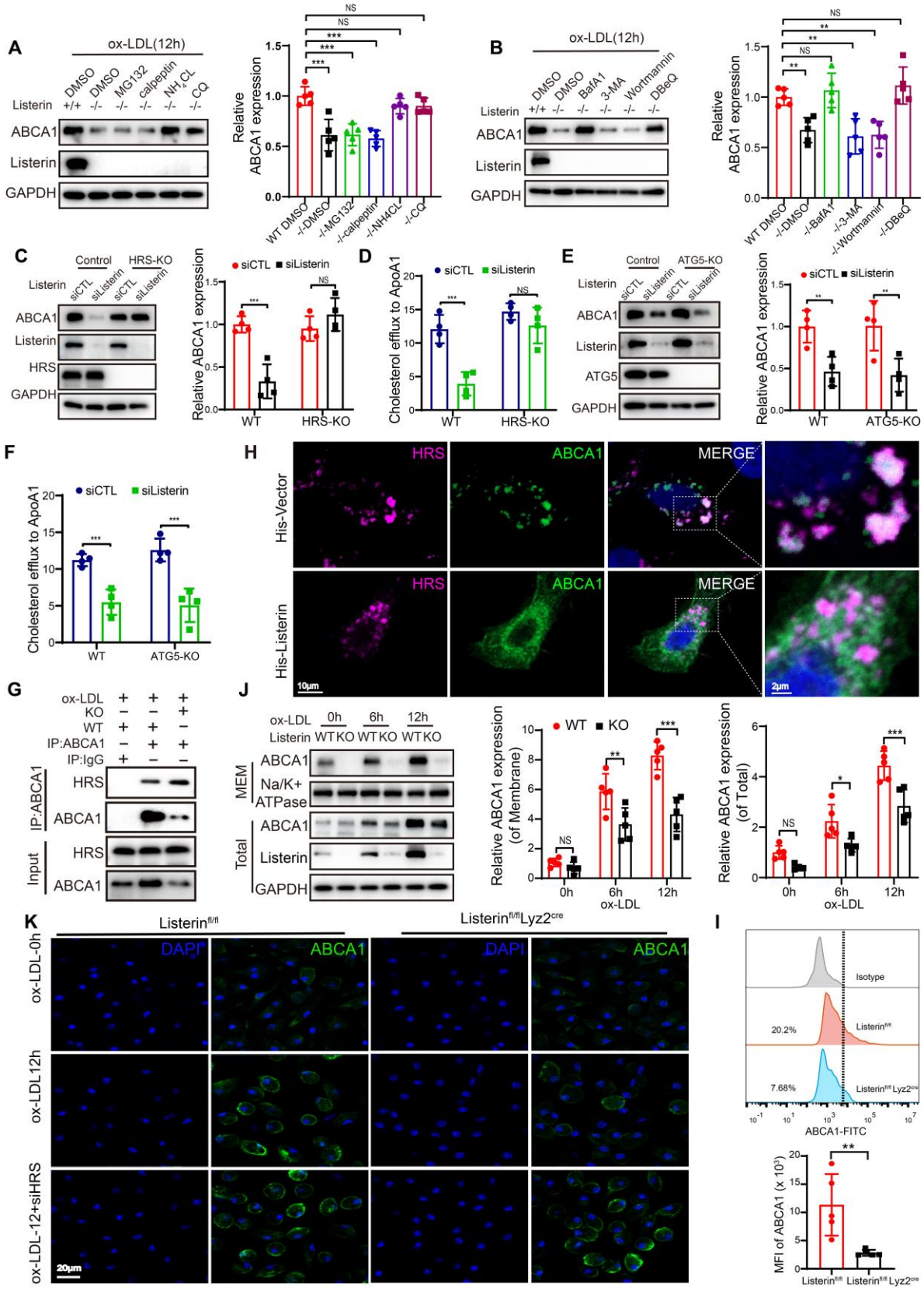

Figure4. Listerin inhibits the degradation of ABCA1 through the ESCRT-lysosomal pathway

(A-B) Immunoblot analysis of ABCA1 expression in PMs from Listerin$^{fl/fl}$ and Listerin$^{fl/fl}$Lyz2^{cre} mice treated with oxLDL (50 μg/ml) and proteasome/lysosome inhibitors (MG132, calpeptin, chloroquine, NH_4Cl, bafilomycin A1, 3-MA, wortmannin, DBeQ). n=5 per group. **(C)** ABCA1 immunoblot in control/HRS-KO THP-1 cells with siCTL/Listerin silencing and oxLDL stimulation. n=4 per group. **(D)** ApoA1-mediated cholesterol efflux in HRS-KO THP-1 cells transfected with siCTL/siListerin. n=4 per group. **(E)** ABCA1 immunoblot in control/ATG5-KO THP-1 cells with siCTL/Listerin silencing. n=4 per group. **(F)** Cholesterol efflux in ATG5-KO THP-1 cells transfected with siCTL/siListerin. n=4 per group. **(G)** Co-IP of ABCA1-HRS interaction in oxLDL-treated PMs. An equal amount of non-specific antibody was used as a negative control. **(H)** Confocal imaging of Flag-HRS/GFP-ABCA1 colocalization with/without His-Listerin overexpression. in Hela cells. Scale bar=10μm. **(I)** Flow cytometry analysis of membrane ABCA1 in PMs from Listerin$^{fl/fl}$ and Listerin$^{fl/fl}$Lyz2^{cre} mice**.** n=5 per group. **(J)** Immunoblot analysis of membrane (MEM) and total ABCA1 in PMs from Listerin$^{fl/fl}$ and Listerin$^{fl/fl}$Lyz2^{cre} mice**.** n=5 per group. **(K)** Confocal microscopic images of ABCA1 in PMs from Listerin$^{fl/fl}$ and Listerin$^{fl/fl}$Lyz2^{cre} mice, PMs silenced HRS and followed by stimulated with oxLDL (50 μg/ml). n=5 per group. Scale bar=20μm. Data were presented as mean ± SD and the Shapiro–Wilk method was used to test the normal distributions. Data analysis was performed with One-way ANOVA followed by Dunnett post hoc test for A, B. Student's *t*-test for I. the others with Two-way ANOVA followed by Sidak post hoc test. For multiple-group comparisons, the adjusted P-values are provided, NS (not significant) $P > 0.05$; *$P < 0.05$; **$P < 0.01$ and ***$P < 0.001$. Each experiment was repeated at least three times independently.

Figure5

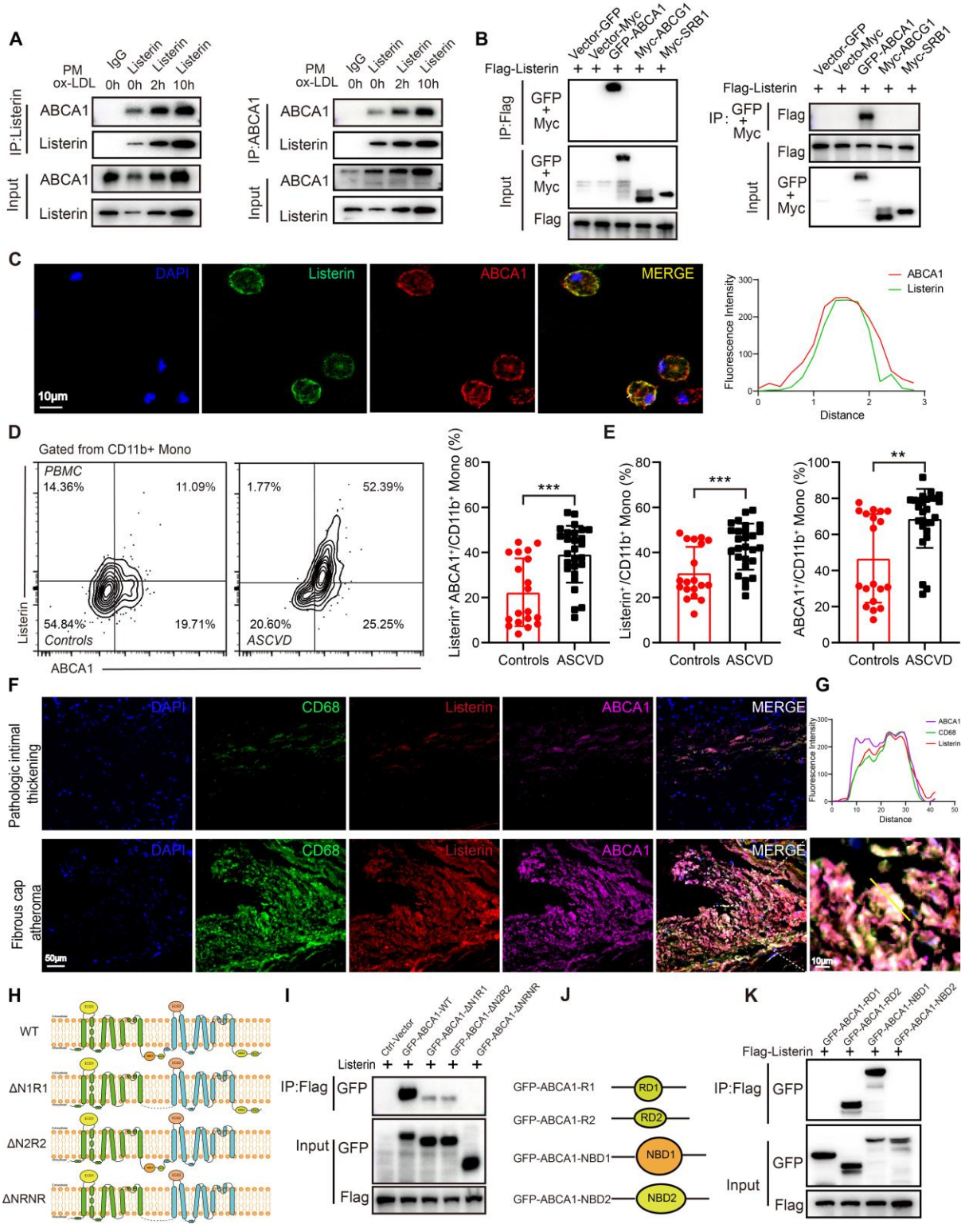

Figure5. Listerin targets ABCA1 **(A)** Co-immunoprecipitation (Co-IP) assay of endogenous Listerin interacts with ABCA1 in PMs treated with oxLDL (50 μg/ml) at the indicated time. An equal amount of non-specific antibody was used as a negative control. **(B)** Co-IP assay of

Flag-Listerin with GFP-ABCA1, Myc-ABCG1, or Myc-SRB1 in HEK293T cells. **(C)** Confocal microscopic images and fluorescence intensity analysis for Listerin and ABCA1 in primary PMs after oxLDL incubation (50 μg/ml). Scale bar=10μm. **(D)** Expression of Listerin and ABCA1 in CD11b+ Monocyte from PBMC of Healthy (n=19) and ASCVD patients (n=27). The graph shows the proportion of $Listerin^{+}ABCA1^{+}CD11b^{+}$ Monocyte among total $CD11b^{+}$ Monocyte. **(E)** Expression of Listerin and ABCA1 is measured in $CD11b^{+}$ Monocyte from PBMC of Healthy (n=19) and AS patients (n=27). **(F)** Immunofluorescence staining of Listerin (red particles), ABCA1(pink particles) and CD68 (green particles) in pathological intimal thickening and fibroatheroma in human coronary artery atherosclerotic plaques. Scale bar=100μm and 10μm. **(G)** Fluorescence intensity analysis for Listerin (red particles), ABCA1(pink particles) and CD68 (green particles) in fibroatheroma in human coronary artery atherosclerotic plaques. **(H, J)** Topological diagram of Human ABCA1 and mutants. **(I, K)** Co-IP assay of the interaction of Flag-Listerin with GFP-ABCA1 (WT) and the ABCA1 truncation mutants in HEK293T cells. Data were presented as mean ± SD and the Shapiro–Wilk method was used to test the normal distributions. Data analysis was performed with Mann-Whitney Test for D and E. For multiple-group comparisons, the adjusted P-values are provided, NS (not significant) $P > 0.05$, $^{**}P < 0.01$, and $^{***}P < 0.001$. Each experiment was repeated at least three times independently.

Figure6

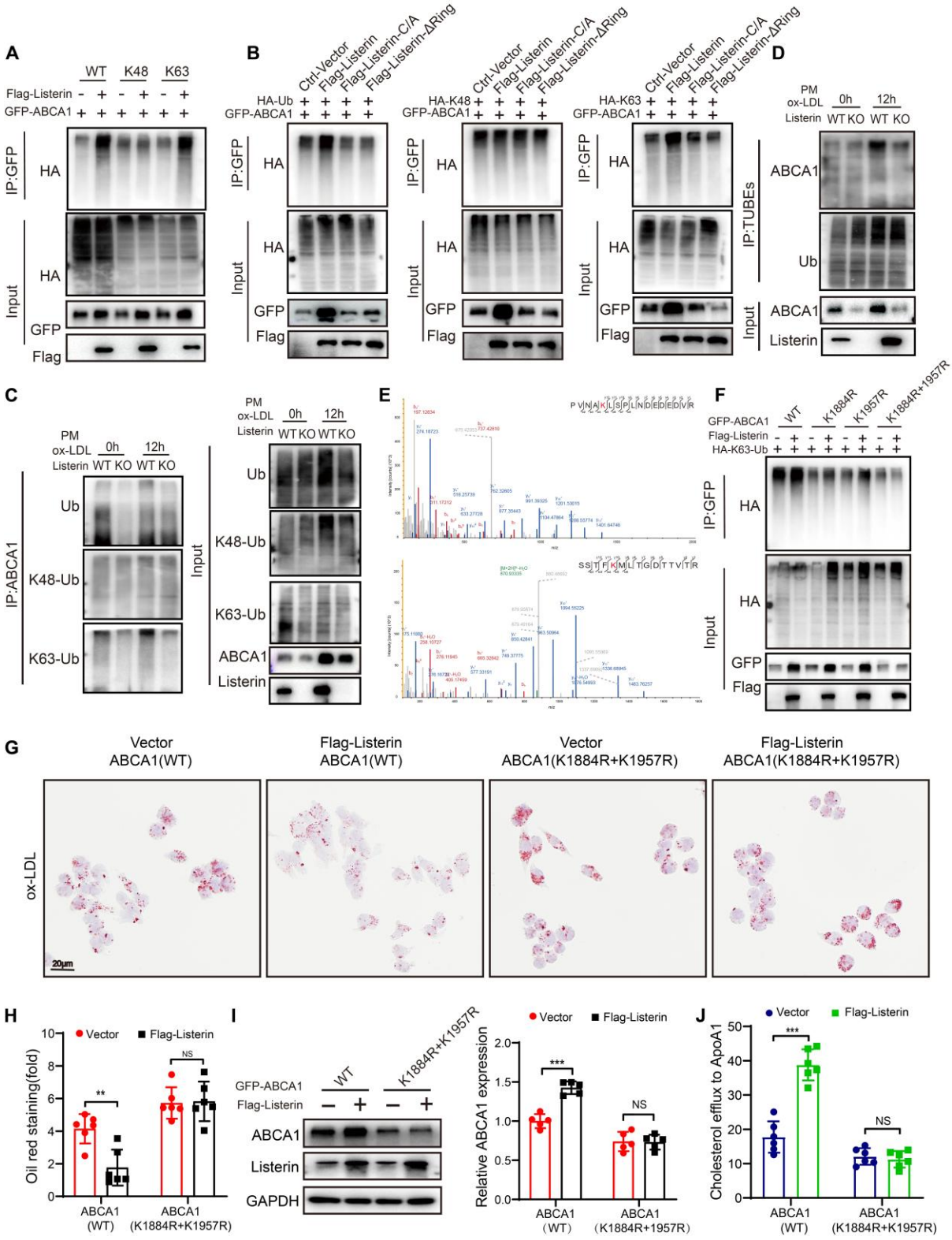

Figure6. Listerin catalyzes K63-linked polyubiquitination of ABCA1 at residues Lys1884 and Lys1957 to inhibit foam cell formation **(A)** Co-IP assay of ABCA1 polyubiquitination in

HEK293T cells transfected with GFP-ABCA1, Flag-Listerin, HA-ubiquitin (WT), or HA-ubiquitin (K48 or k63). **(B)** Co-IP assay of ABCA1 polyubiquitination in HEK293T cells transfected with GFP-ABCA1, HA-ubiquitin (WT), HA-ubiquitin (K48 or K63), as well as a control vector, Flag-Listerin (WT), Flag-Listerin-(C/A), or Flag-Listerin-ΔRing. **(C)** Co-IP assay of endogenous ABCA1 polyubiquitination in PMs from Listerin$^{fl/fl}$ and Listerin$^{fl/fl}$Lyz2^{cre} mice after being stimulated with oxLDL for 12 h. **(D)** Co-IP assay of ABCA1 polyubiquitination after ubiquitin (TUBE) pull-downs in PMs. **(E)** LC-MS spectra analysis identifies the ubiquitin modification of ABCA1 at lysine residues K1884, and K1957. **(F)** Co-IP analysis of the polyubiquitination of ABCA1(WT) and its mutants in HEK293T cells transfected with GFP-ABCA1 (WT or mutants), Flag-Listerin, and HA-ubiquitin(K63). **(G)** Oil red O staining images and quantitation analysis **(H)** of RAW264.7 macrophages transfected with Flag-Listerin and GFP-ABCA1(WT) or GFP-ABCA (K1884R and K1957R), then incubated with oxLDL (50 μg/mL) for 24 hours. n=6 per group. Scale bar=20μm. **(I)** Immunoblot analysis of GFP-ABCA1 and GFP-ABCA1(K1884 and K1957) expression in RAW246.7 macrophages. n=5 per group. **(J)** ApoA1-mediated cholesterol efflux assay of RAW246.7 macrophages transfected with Flag-Listerin, GFP-ABCA1, or GFP-ABCA1(K1884 and K1957). n=6 per group. Data were presented as mean ± SD and the Shapiro–Wilk method was used to test the normal distributions. Data analysis was performed with Two-way ANOVA followed by the Sidak post hoc test. For multiple-group comparisons, the adjusted P-values are provided, NS (not significant) $P > 0.05$, $^{**}P < 0.01$, $^{***}P < 0.001$. Each experiment was repeated at least three times independently.

Figure7

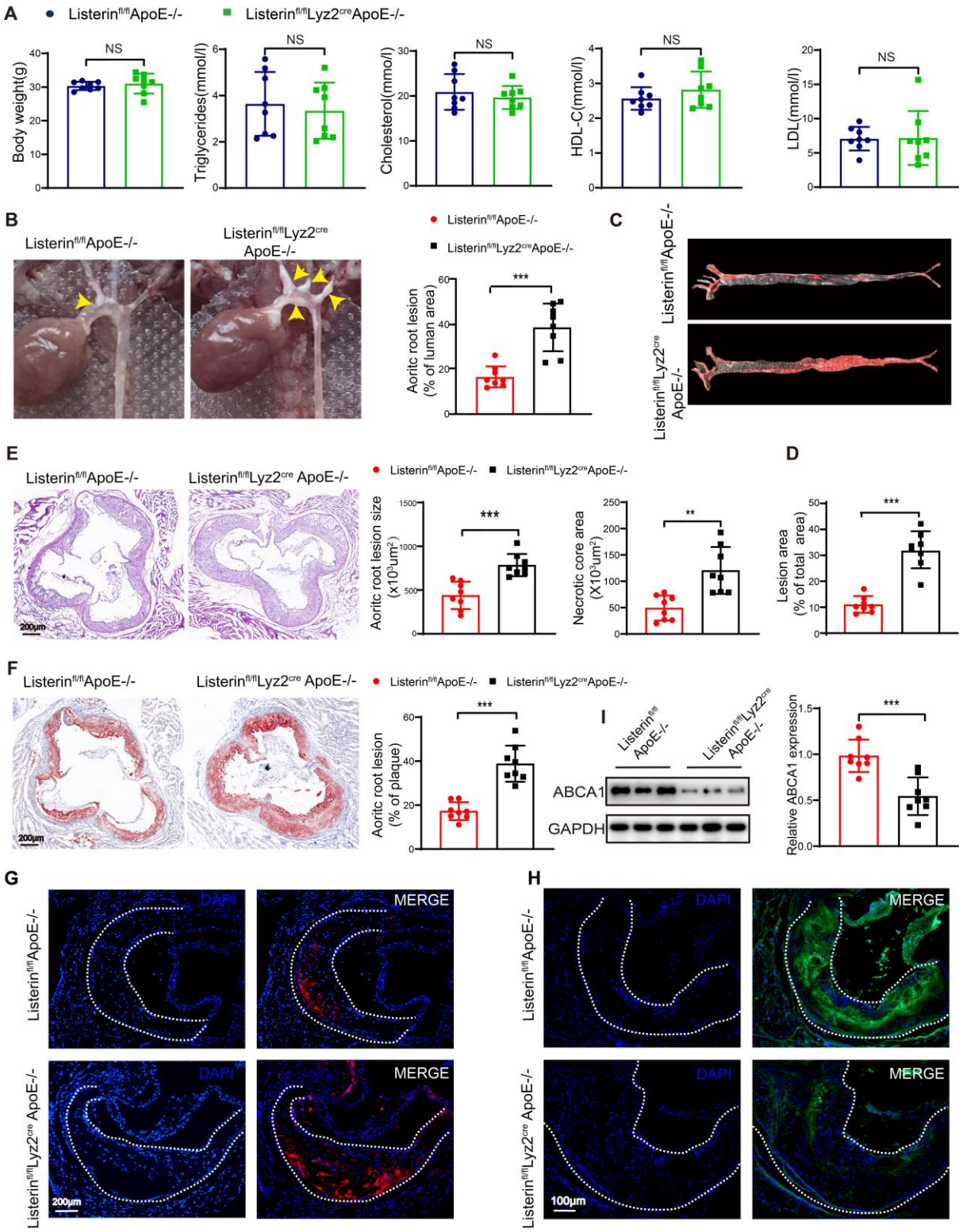

Figure7. Listerin knockout aggravates the development of atherosclerosis in vivo

Male ApoE-/- Listerin$^{fl/fl}$ and ApoE-/- Listerin$^{fl/fl}$ Lyz2^{cre}mice were fed a Western diet for 16

weeks. **(A)** The measurement of Body weight and serum levels of triglycerides(mmol/l), cholesterol(mmol/l), HDL-C(mmol/l), and LDL (mmol/l). n=8 per group. **(B)** Representative images and quantitation of aortic arch regions containing white plaques (yellow arrows). **(C)** En face Oil red O staining and quantitation **(D)** of atherosclerotic plaques in the whole aorta. n=8 per group. **(E)** H&E staining of representative aortic root sections, quantification of lesions area and necrotic core area. n=8 per group. Scale bar=200μm. **(F)** Oil red O stained cross sections analysis of atherosclerotic plaques in the aortic root. n=8 per group. Scale bar=200μm. Immunofluorescence staining of CD68 **(G)**, and ABCA1 **(H)** in aortic root. n=8 per group. Scale bar 200μm. **(I)** Immunoblot images and quantitative analysis of ABCA1 in the whole-aorta lysates from ApoE-/- Listerin$^{fl/fl}$ and ApoE-/- Listerin$^{fl/fl}$ Lyz2^{cre}mice, n=8 per group. Data were presented as mean ± SD and the Shapiro–Wilk method was used to test the normal distributions. Statistical analysis was performed by Student's *t*-test. ***P < 0.001.

Figure8

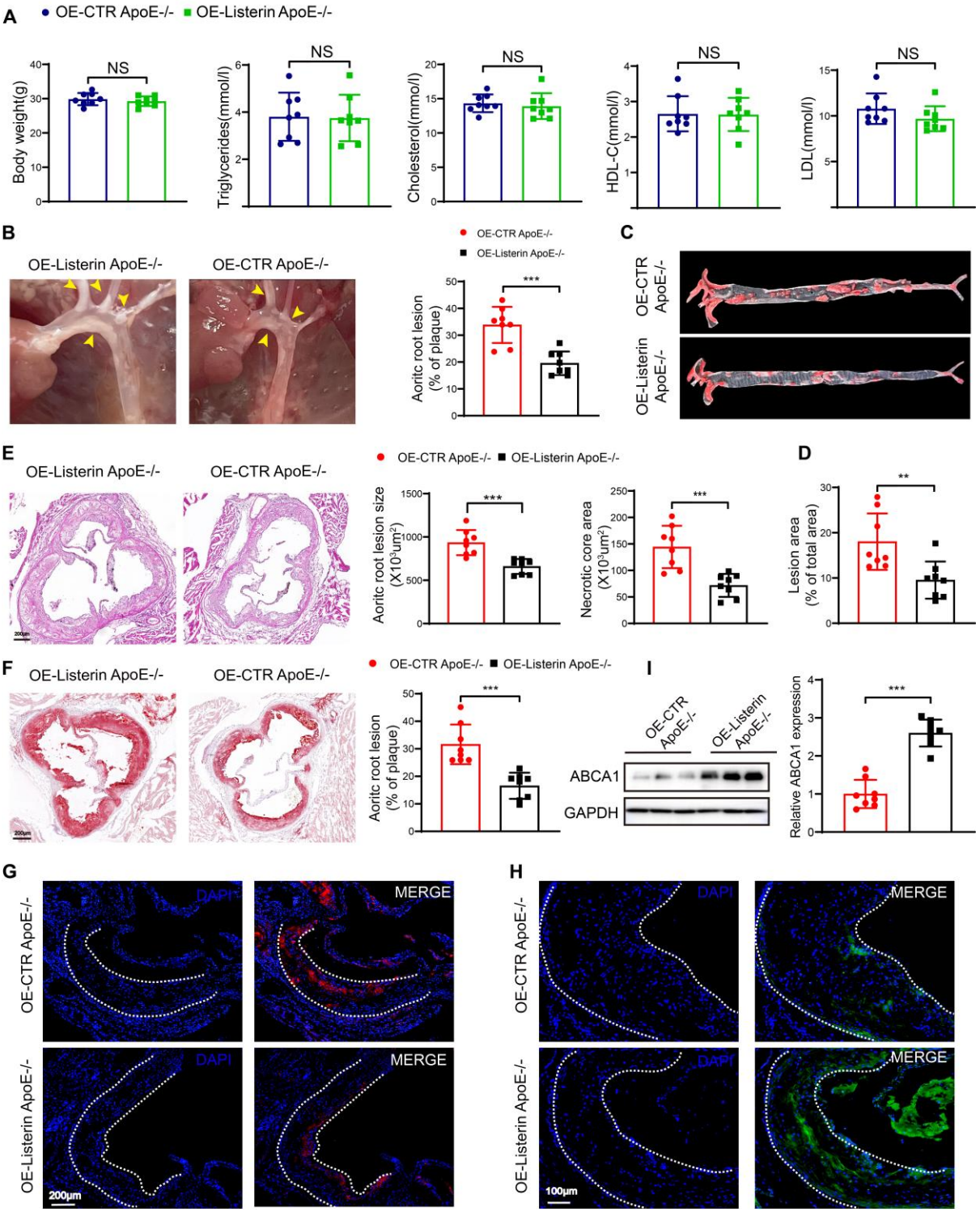

Figure8. Listerin overexpression ameliorates the development of atherosclerosis in vivo **(A)** The measurement of Body weight and serum levels of triglycerides(mmol/l), cholesterol(mmol/l), HDL-C(mmol/l), and LDL (mmol/l). n=8 per group. **(B)** Representative

images and quantitation of aortic arch regions containing white plaques (yellow arrows). **(C)** En face Oil red O staining and quantitation **(D)** of atherosclerotic plaques in the whole aorta. n=8 per group. **(E)** H & E staining of representative aortic root sections, quantification of lesions area and necrotic core area. n=8 per group. Scale bar=200μm. **(F)** Oil red O stained cross sections analysis of atherosclerotic plaques in the aortic root. n=8 per group. Scale bar=200μm. Immunofluorescence staining of CD68 **(G)**, and ABCA1 **(H)** in aortic root. n=8 per group. Scale bar=100μm and 200μm. **(I)** Immunoblot images and quantitative analysis of ABCA1 in the whole-aorta lysates from OE-CTR ApoE-/- mice and OE-Listerin ApoE-/- mice, n=8 per group. Data were presented as mean ± SD and the Shapiro–Wilk method was used to test the normal distributions. For the comparison between the two groups, the Student's t-test is used if the data is normally distributed, and the Mann-Whitney Test is used if not. **P < 0.01, ***P < 0.001.